Physics–Uspekhi 39 (4) 337–362 (1996)

REVIEWS OF TOPICAL PROBLEMS

PACS number: 87.10.+e

Synchronisation in neural networks

H D I Abarbanel, M I Rabinovich, A Selverston, M V Bazhenov,
R Huerta, M M Sushchik, L L Rubchinskiĭ

Contents

Abstract. **The construction of a dynamical theory of neural networks has been a goal of physicists, mathematicians and biologists for many years now. Experimental breakthroughs in modern neurobiology have allowed researchers to approach this goal. Significant advances have been made for small neural networks, which are generators of the rhythmic activities of living organisms. The subject of the present review is the problem of synchronisation, one of the major aspects of the dynamical theory. It is shown that synchronisation plays a key role in the activity of both minimal neural networks (neural pair) and neural assemblies with a large number of elements (cortex).**

1. Introduction

1.1 Historical background

Classical concepts of the synchronisation phenomenon are based on the notions of closeness of the frequencies or phases of the subsystems generating periodic oscillations. A pendulum clock fastened to a beam (Huygens [1]), acoustically coupled organ pipes (Rayleigh [2]), electronic generators (Van der Pol [3], Andronov, Vitt [4]), different modes in a laser cavity, Josephson junctions forming an array [5] are all examples of such subsystems. This list may be continued.

Using the traditional language of dynamical systems with continuous time one can say that synchronisation of periodic oscillations may be represented as follows. While a stable limit cycle is a geometrical image of such oscillations, an attracting two-dimensional (or n-dimensional) torus is a geometrical image of the oscillations generated by two (or n) uncoupled oscillators in a common phase space. As the parameter of coupling is increased ($\epsilon > 0$), the motions of partial subsystems are no longer independent, and a stable limit cycle is born on the torus that is still an attractor. This corresponds to the transition of the system to synchronisation.

More detailed information about the synchronisation and resonance phenomena in a system of two coupled oscillators possessing regular dynamics is furnished by devil's staircase (the rotation number of the system on a torus plotted versus frequency of one of the oscillators). The rotation number is the limiting ratio $\varphi_1(t)/\varphi_2(t)$ of the phases of partial oscillators which were independent at $\epsilon = 0$: $\mu(\epsilon) = \lim_{t\to\infty}[\varphi_1(t)/\varphi_2(t)]$. For unidirectional coupling, i.e., when a periodic force of frequency ω_2 acts on an oscillator of frequency ω_1, the dependence of the rotation number on ω_2 has a form of a staircase whose steps form a Cantor set. The rotation number equal to the ratio of integers, $\mu = p/q$, corresponds to synchronisation. The numbers p and q correspond to the numbers of the harmonics at which

H D I Abarbanel, A Selverston, R Huerta
University of California, San Diego, USA
M V Bazhenov, M M Sushchik, L L Rubchinskiĭ Institute of Applied Physics, Russian Academy of Sciences, ul. Ul'yanova 46, 603600 Nizhniĭ Novgorod, Russia. Tel. (7-8312) 36 72 91
M I Rabinovich University of California, San Diego, USA, Institute of Applied Physics, Russian Academy of Sciences, ul. Ul'yanova 46, 603600 Nizhniĭ Novgorod, Russia
E-mail: rabin@gibbs.ucsd.edu

Received 10 October 1995
Uspekhi Fizicheskikh Nauk 166 (4) 363–390 (1996)
Submitted in English by the authors; edited by S D Danilov

synchronisation occurs. If one follows the changes not only of the frequency ω_2 but also of some other parameter, for example, force amplitude γ, then the synchronisation regions are no longer sections on the curve line ω_2 but, instead, regions on the plane (γ, ω_2). Usually these regions are tongue-shaped and are referred to as the Arnol'd tongues [6].

Synchronized motions in organisation of coupling are inherent in both periodic and chaotic oscillators. A strange attractor is a geometrical image of such partial oscillations. A typical feature of coupled non-identical chaotic subsystems is that they can coordinate their motions only on the average in time [7]. Chaotic synchronisation may result in identical topologies of strange attractor projections onto partial subspaces, identical correlation dimensions and power spectra of partial oscillations. Being similar in a certain sense, the time series, however, need not necessarily to coincide locally in time.

In this situation it is natural to introduce the concepts of generalised synchronisation and degree of synchronisation. They are particularly important as applied to synchronisation of the neurons generating rather complex pulsations with several characteristic time scales.

Typical oscillations generated by a pacemaker are shown in Fig. 1. They may be chaotic or regular, but, generally, one can distinguish bursts of spikes alternating with a relatively slow variation of membrane potential. One can speak about synchronisation, for instance, of slow motions considering only bursts, or about complete synchronisation when, besides bursts, spikes are also regarded.

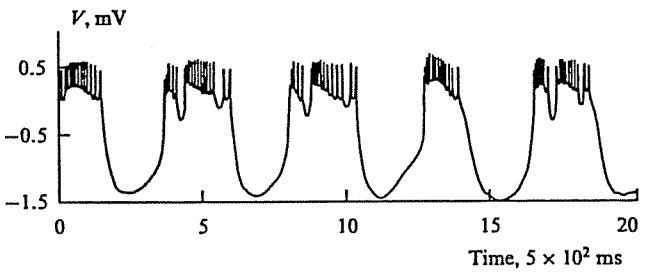

Figure 1. Time series from an isolated real neuron. It has been measured from a stomatogastric LP neuron of CPG of lobster, when the rest of the neurons in the ganglion has been hyperpolarised [40].

Early investigations of synchronisation in neural networks concerned analysis of the behaviour of central pattern generators (CPG) which control rhythmic movements of living organisms (breathing, walking, running, etc.). Different dynamical models of neuron-oscillators, including those described by symbolic dynamics (finite automata) were employed. One of the pioneer works in this field described the synchronised (with the constant phase shift taken into account) work of the CPGs controlling the locomotion of salamanders in terms of finite automata [8].

Today, it is common knowledge supported by numerous experiments (see Section 4) that rhythmic movements of living organisms are governed by the CPGs which generate a standard rhythm in an autonomous regime too, i.e., without making use of the sensory feedback with the moving organs of the animal. Nevertheless, such a feedback plays a very important role when environmental conditions are changed. This feedback changes the internal rhythmic pattern of CPG.

Investigations into the dynamics of CPGs of small neural networks have radically changed our understanding of the cooperative behaviour of neurons in ensembles. The basic principles of synchronous operation of coupled neurons were revealed: the mechanisms responsible for the formation of stable regimes with a fixed phase shift between the interacting neurons (e.g., for the CPG governing the rhythm of swimming of a lamprey), the ability of such systems to learn to be synchronised, and others. Of great significance are advances in experimental methods which now allow one to obtain rather long time series for oscillations of individual neurons and use for processing of the results a broad variety of techniques available in nonlinear dynamics today: analysis of the Lyapunov exponents, calculation of the mutual information function, etc. [9–11]. We believe that the experimental data obtained in analysis of different CPGs controlling the rhythmic activity of invertebrates and elementary vertebrates will enable researchers to answer, in the near future, the basic questions related to synchronisation and stable operation of small neural networks.

The situation is quite different when we speak about the mechanisms of cooperative work and synchronisation of neurons in large neural networks (e.g., $N \sim 5 \times 10^9$ in the human cortex). Analysis of such complex systems cannot be based on direct experiments (whereas indirect ones may be treated ambiguously). So, basic knowledge, in this case, is gained by constructing models which merely illustrate whether one or another problem may be solved in principle, i.e., they may suggest a possible scenario of its solution in the living cortex. In the context of this overview, the most significant achievement in the recent years is the discovery in neurophysiological experiments of the fact that the phenomenon of perception may be closely related to oscillatory activity of neurons, including the cases when this activity was stimulated by non-oscillatory sources. This is true for both individual neurons and neuron populations (see Section 5).

1.2 Neuron models

A nerve cell and a cellular membrane are shown schematically in Fig. 2. For construction of an adequate dynamical model of a neuron it is essential that the surrounding membrane is frequently an equipotential surface. Therefore, in analysis of electric activity (the frequency of 4 to 60 Hz) of neurons, in spite of their macroscopic size, nerve cells may be regarded as a system described by ordinary differential equations. In other words, the variables describing the state of the neuron (membrane potential, ionic concentration, and so on) may be considered as functions of time only. Another important issue is description of neural activity. The state of the neuron is determined by nonequilibrium diffusion of different charged ions. Consequently, its activity should be modelled, generally speaking, using a kinetic description. However, there is no need for such a description when we are interested in a neuron as a generator of low-frequency electric pulsations. For construction of an adequate theory it suffices to employ equations for dynamical variables: membrane potential and macroscopic ionic currents averaged over time $t_0 \ll T$ (T is the characteristic period of electric activity of the neuron). The neuron can then be regarded as a nonlinear electric circuit of RC elements (see Fig. 2c). Biochemical processes associated with the interaction of intracellular and intercellular media (see, e.g., Ref. [12] for detail) are energy sources for operation of this dissipative system.

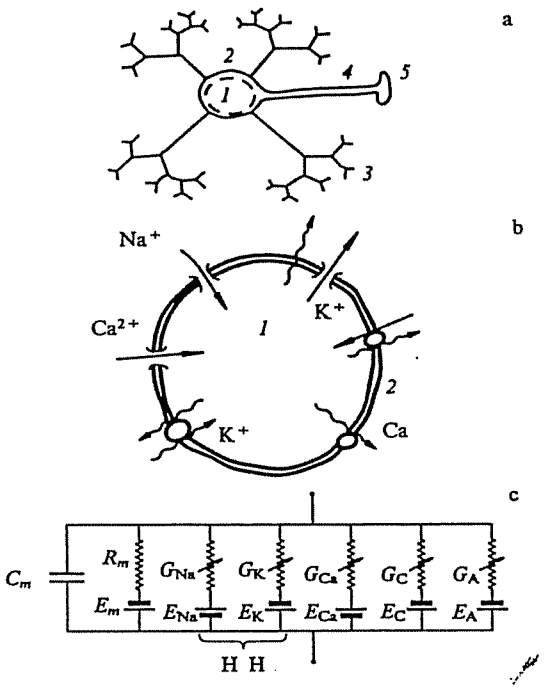

Figure 2. (a) Schematic picture of a neuron: *1* — soma, *2* — membrane, *3* — dendrites, *4* — axon, and *5* — synaptic terminals. (b) Ionic channels in neuron membrane: K — potassium ions, Na — sodium ions, Ca — calcium ions. (c) Electronic circuit which models the neuron membrane: G_{Na}, G_K, G_{Ca}, ... — nonlinear ionic conductances; R_m — leaking resistors; C_m — membrane capacitance; E_{Na}, E_K, ... — rest potentials for each ionic currents.

It is a nonequilibrium system with various feedbacks, including delayed ones, which determines oscillatory activity of neuron. Thanks to these feedbacks that open or close ionic channels of the membrane at the respective phase of electric activity the state of the neuron, corresponding to the rest potential, may become unstable and the neuron becomes a generator. Such a generator may be regarded as a dynamical system in the framework of which microscopic kinetics is seen only as small fluctuations.

The choice of nonlinear dynamical models of neurons that are constructed for explanation of known phenomena and prediction of new ones (which is, actually, the purpose of any theory) depends to a great extent on the neurophysiological experiment. For example, CPG neurons are usually described by variants of the classical Hodgkin–Huxley model (1952), including its numerous generalisations which take into account additional membrane currents; or, on the contrary, more simplified models that use as variables membrane potential $V(t)$ and some auxiliary currents describing processes of two types: fast $I_f(t)$ and slow $I_s(t)$ ones (see, e.g., Refs [13–15]).

A typical generalised Hodgkin–Huxley model (in a broader sense, a conductance-based model) is written in the form

$$C\frac{dV}{dt} = I - \sum_{i=1}^{N} g_i a_i^{p_i}(t) b_i^{q_i}(t)\left[V(t) - V_i\right],$$

$$\frac{da_i}{dt} = \frac{a_{\infty_i}(V) - a_i}{\tau_{a_i}(V)},$$

$$\frac{db_i}{dt} = \frac{b_{\infty_i}(V) - b_i}{\tau_{b_i}(V)}, \quad i = 1,2,3,\ldots,N, \tag{1.1}$$

where $V(t)$ is the electric potential of cellular membrane, C characterises the electric capacitance of the membrane, i designates the type of the current flowing through the membrane or, in other words, the ion channel (potassium, sodium or calcium channel, leakage channel), g_i is the maximal conductivity, V_i is the equilibrium potential (reverse potential) for the i-th channel, a_i and b_i are the variables describing activation and inactivation of the i-th channel which can be regarded, for instance, as the probability of opening or closing one or another channel; p_i and q_i are the numbers of the controlling particles that are sufficient to open or close the channel (usually, these are integers ranging from zero to four); and $a_{\infty_i}(V)$ and $b_{\infty_i}(V)$ are stationary states of the activation and inactivation levels. They have a sigmoid dependence on V, as characteristic relaxation times $\tau_{a_i}(V)$ and $\tau_{b_i}(V)$. In the classical work of Hodgkin and Huxley $N = 3$ [14].

Simpler models of this type are also popular today. One of the simplest is the Morris–Lecar model [15]:

$$\frac{dV}{dt} = -g_{Ca} m_\infty(V)(V - V_{Ca}) - g_K W(V - V_K),$$

$$\frac{dW}{dt} = \frac{\lambda\left[W_\infty(V) - W\right]}{\tau(V)}, \tag{1.2}$$

where $m_\infty(V)$, $W_\infty(V)$, and $\tau(V)$ are sigmoid functions. Only one variable W describing neuron activation is taken into consideration here. Of course, it is impossible to describe all details of neuron dynamics including chaotic oscillations of the membrane potential of the cell observed in different experiments [16, 17] in the frames of a dynamical model with two-dimensional phase space, since the strange attractor cannot be embedded into two-dimensional space. Therefore, three-dimensional models based on the Hodgkin–Huxley formalism are rather popular too, for example, the Chay model [18] and some others.

The Hodgkin and Huxley formalism that is based on a detailed analysis of ionic transport through the membrane has proved to be very successful and is broadly employed today. However, phenomenological models describing typical features of neuron dynamics are also highly productive. A popular model of this type is the Rose–Hindmarsh model [19] (see Section 3 for more detail):

$$\frac{dx}{dt} = y + ax^2 - bx^3 - z + I,$$

$$\frac{dy}{dt} = c - dx^2 - y,$$

$$\frac{dz}{dt} = r\left[s(x - x_0) - z\right], \tag{1.3}$$

where x is the membrane potential, y characterises 'fast' currents (e.g., potassium and sodium ones), z describes 'slow' currents, I is an external current, and a, b, c, d, r, s, and x_0 are constant parameters.

The Wilson–Cowan model (1972) is popular in analysis of dynamical processes in the cortex. This model describes oscillations in a system of two coupled neuron populations, inhibitory and excitatory ones [20]:

$$\frac{dE}{dt} + E = F_E(f_e E - f_i I - P),$$
$$\frac{dI}{dt} + \epsilon I = \epsilon F_I(g_e E - g_i I - Q), \quad (1.4)$$

where E and I are the dimensionless variables characterising the activity of excitatory and inhibitory neurons, respectively; $\epsilon < 1$ because the time constants for inhibition are usually larger than the characteristic excitation times; and F is a sigmoid function: $F = 1/(1 + e^{-x})$ or $F = 1/2 + (1/\pi)\arctan x$.

Very simple models in the form of phase oscillators (see, e.g. Refs [21, 22])

$$\frac{d\Theta_i}{dt} = \omega_i + \epsilon \sum_{j=1}^{N} H_{ij}(\Theta_i, \Theta_j) \quad (1.5)$$

or still simpler spin type models, like the ones popular in the theory of phase transitions, are also used for modelling large neural networks. The scope of our overview does not allow us to analyze even briefly all the numerous models of neurons available today. Information about them is summarised in Table 1 (see Conclusions).

A particular role in the construction of a dynamical theory of neural networks belongs to models of synaptic couplings between neurons. Their properties should be considered in more detail.

2. Why does the synchronisation in neural networks differ from the synchronisation of physical oscillators?

The nerve cells which have evolved in higher organisms are actually very complex biochemical systems. The genes and the biochemical arrangement of neurons are in many ways similar to that found in other cells, but they also have a number of characteristic features which distinguish them from all the other cells in the animal. They are not divided in the post-embrional period (i.e. they cannot be a building material), do not produce energy for organism, do not carry mechanical loads. Their distinctive feature that is typical of neurons only is the ability to process information. They are able to generate electrical oscillations (single pulses — rest potentials or their sequences) Another typical feature is original architecture: the body of the cell and pronounced branches (axon and dendrites connecting the neurons). One of the most important controlling factors within the central nervous system is the synapse (Fig. 2). In this section we will discuss its important roles by examining the result of combining synapses into small networks and the effect that synapses have on neural synchronisation.

2.1 Synapse. Synaptic delay in neural networks

There are two causes for the delay in the coupling between neurons. The first one is due to the cable properties of the neuron, which is not specific of biology. A typical delay varies from 0.5 ms (a short axon) to tens of milliseconds (a very long axon) in transmission along the axon and dendrites. In many long axons the speed of transmission is also affected by the presence of a myelin sheath and the saltatory connection which occurs between the nodes of the sheath. The speed of transmission in myelin nerve fibers is 5—10 times greater than in non-myelin ones. The second cause for delay is synapse. To better understand the mechanism of synaptic delay, we will describe how the synapse is organised [12, 23, 24].

Synapses (see Fig. 3) consist of two elements, the presynaptic terminal and the postsynaptic receptor site, which may be located on the axon, soma or dendrite of the nerve cell. The two elements are separated by a synaptic cleft. There exist synapses of two types: electrical and chemical ones. There is almost no delay in electrical synapse. The ions flow in or out of the nerve cells connected with each other. The electrical coupling that occurs through this synapse results in levelling of membrane potentials, i.e. in a decrease of the error signal $V_j - V_i$. The electrical synapses provide excitation in either direction (reciprocal coupling). Such a coupling plays a decisive role in synchronisation of the activity of different groups of neurons in some invertebrates (e.g., a leech).

In a chemical synapse, the information is transmitted through intercellular space (the cleft between presynaptic and postsynaptic membranes is about 150—200 Å, that is an order of magnitude higher than in the electrical synapse). The presynaptic terminals contain neurotransmitters which are packaged into synaptic vesicles. Typical neurotransmitters are glutamate and its derivatives and GABA which cause excitation or inhibition, respectively. When an action potential invades the presynaptic terminal, the neurotransmitter is released through the presynaptic membrane into the synaptic cleft. When the neurotransmitter binds to the postsynaptic membrane, the permeability and, consequently, the membrane potential change.

Apparently, the synaptic delay is the result of the chemical synapse of neurotransmitters. The typical delay time is 0.3–1 ms. This time is spent primarily on the neurotransmitter release in the presynaptic terminal.

It should be noted that the delay time is not constant in real neural networks. For example, enhanced activity of neuron population decreases the delay time, which increases susceptibility of the neural network [25] and has a positive effect on the processes of attention, short-term memory and learning which occur at enhanced neuron activity.

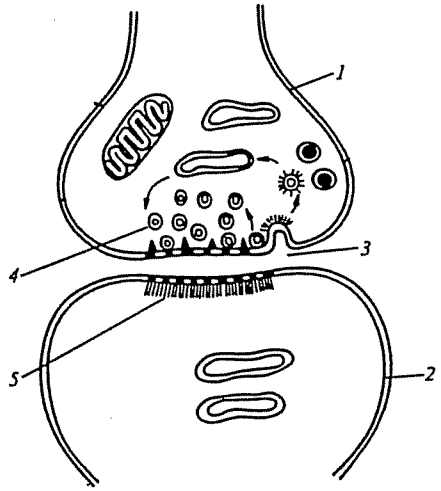

Figure 3. Sketch of a chemical synapse: *1* — presynaptic membrane, *2* — postsynaptic membrane, *3* — intercellular space, *4* — vesicles, *5* — postsynaptic receptors.

2.2 Syncronisation and state changes

Neural networks have been shown to have different dynamical properties depending on their biochemical environment. This environment is shaped by hormones as well as neuromodulatory chemicals released by specific neurons. Particular substances can change the operating state of the neural system which in terms of nonlinear dynamics is associated with multistability. A specific stable synchronous behaviour of neurons (e.g., having different phase shifts between the synchronised neurons) may correspond to each regime of operation of the system. This property is readily illustrated by a relatively simple example: a CPG. Such a generator is a group of synaptically coupled neurons generating sets of different patterns for controlling motor activity. Here we will consider a CPG controlling the locomotion of a horse (see Section 4 for detail). It is known that a horse may stride, trot, gallop or pace, depending on the speed at which it moves its limbs. A model for such a CPG [22] is a network comprising 4 pacemakers. In the simplest approximations, such neurons may be regarded as phase oscillators (see Section 4.3). In the framework of such a model different gaits correspond to different stable phase shifts between the oscillators responsible for locomotion. Co-existence in phase space of several attractors enables the neural network to change its behaviour, without parameter changes, under the action of even a short signal that emerges as the conditions are changed.

2.3 Plasticity and learning

Learning may be defined as an adequate variation of the parameters of neural networks whose purpose is to perform (acquire) new functions, which is assured by a relevant signal. This property is also referred to as plasticity. Unlike multistability, plasticity is connected with restructuring of dynamics of the neural network that occurs as a result of parameter changes. Multistability and plasticity co-exist in living mechanisms.

Learning, at the cellular level, is based on the ability of synapses to change their parameters under different conditions. If synapses are in an active state for a rather long time (i.e., presynaptic and postsynaptic cells are excited simultaneously), then the efficiency of signal transmission can be increased. Such a synaptic memory is due to the complex biochemical mechanisms of synapses [24, 26, 27]. In particular, electrical [28] and chemical [29] feedbacks may be engaged. This process can be described, at the biochemical level, as follows. When some stimulus acts on the postsynaptic neuron, there is an inflow of positively charged ions that leads to a decrease of the membrane potential. The calcium channels open and Ca^{2+} ions invade the cell. These ions activate some enzymes, including those causing rearrangement of the proteins forming the membrane. The ion channels are modified in the membrane, the signal from the presynaptic neuron excites the postsynaptic neuron more effectively, and the synaptic coupling is enhanced. For a relatively long action on the brain of some stimulus, the synaptic couplings change so that a whole class of close stimuli fix these couplings (memorising). A distinctive feature of such a memory is associations. If the image memorised by the neural network is represented with distortions, it will recognise it all the same, i.e., the memory compares the computed image with the one of the original image it has memorised. Memorising the couplings between different stimuli (as in conditioned reflexes, etc.) is even more complicated. Complicated processes of reciprocal action of closely located synapses, each of which is excited by one of the stimuli, makes the basis for such memory. Strictly speaking, when real neural networks are taught, not only synapses but also neurons are changed. In this connection, it is interesting to mention the following experimental fact [26]. If the neurons of new-born animals are pharmacologically blocked so that they are not capable of firing action potentials, then these neurons and their synapses cannot change (develop) as in a normal brain.

Such experiments allowed researchers to formulate some rules about learning. The simplest of them is Hebb's rule [30, 31] which reads as follows: The synaptic coupling S_{ij} between the i-th and j-th neurons is enhanced if the stimulus simultaneously enhances activity of these post- and presynaptic neurons. (It is natural that this rule needs to be modified in the case of inhibitory coupling.) This rule is frequently employed for teaching one of the simplest neural networks — Hopfield's network [32], in which the neuron may be in two states only. On completion of learning, the network is capable of recognising images. Naturally, learning, memorising, and the processes of recognition and forgetting occur simultaneously in living neural networks, but within different time scales.

An adequate model for neural networks must include dynamical equations for the parameters of synaptic couplings. An example of an equation for synaptic coupling is [33]

$$\frac{dS_{ij}}{dt} = \alpha I_i \sum_n \delta(t - t_n^j) - F, \tag{2.1}$$

where I_i is the current flowing into the cell i, t_n^j is the time of pulse generation in the j-th cell, α is a positive parameter the variations of which may allow for the action of neurotransmitters (neuromodulators), and F characterises forgetting. Such adequate self-consistent models for neural networks are still to be constructed.

2.4 Self-regulation

A reliable neural network must function safely and steadily when the input signals fluctuate or some neurons fail, which is of fundamental significance because the nerve cells are not restored. This means that the neural network must be structurally stable in a broad sense. At the same time, if external changes are substantial, the network must develop dynamically to match these changes. Self-modulation is one of the possible mechanisms responsible for such a behaviour. The self-modulation is generation by the neural network of neuromodulators, i.e., chemically active substances which change (modulate) the property of synapses by weakening or strengthening the action of neuromediators (for example, by blocking their generation, destroying them, blocking the postsynaptic membrane or, on the contrary, preventing their destruction, and so on).

Self-modulation may be both short-and long-term one. Short-term modulation is especially typical of small neural networks (or CPG). In particular, it is inherent in stomatogastric CPG of a lobster [34] (see also Section 3), swimming CPG of a clione [35], swimming CPG of a tritonia [36], and so on.

Long-term self-regulation is observed, in particular, in hypocampus neurons responsible for the functions of memory in the cortex [37]. Recent experiments showed that such a mechanism connected with the action of neuromedia-

tors released by a neuron on its neighbouring neurons also influences the learning process [38].

3. Synchronisation of chaotic neurons

3.1 'Living' neurons' and strange attractors

Experiments performed in recent years at different laboratories [16, 17, 39, 40] indicate that normal activity of a single neuron is dynamical chaos.† For instance, one of typical time series of the membrane potential of a single neuron of lobster's CPG is given in Fig. 1 [40]. Analysis of a rather long time series (duration of about 1 min) confirms that the given chaotic series is, actually, generated by a dynamical system. In other words, the observed chaos is a consequence of the dynamics inherent in the neuron and is not caused by noise. The phase portrait of a limit cycle (a strange attractor in this case) reconstructed from this time series is presented in Fig. 4a. One can see that the strange attractor is embedded into three-dimensional phase space. The low dimension of the chaotic signal generated by lobster's neuron is also verified by direct calculations of the Lyapunov exponents. Such a series possesses only one unstable direction ($\lambda_+ \approx 1.5$, $\lambda_- \approx -2.0$) (Fig. 4b). Thus, the Lyapunov exponent of the time series D_λ is approximately equal to 2.75, which does not contradict possible embedding of the reconstructed attractor into three-dimensional space.‡

Similar results follow from experiments on a single neuron, pacemaker of the Onchidium mollusc [16], as well as on other neurons (see the literature cited in Ref. [39]).

Observation and confirmation of the fact that an individual neuron is a dynamical system generating chaotic pulsations give rise to many questions. What mechanisms are responsible for regular (or, at least more ordered) behaviour of small neural networks and why? We expect that the dynamics of an ensemble of chaotic oscillators must be more complicated (certainly not simpler), than that of a single chaotic neuron. What is the minimal number of chaotic neurons in CPG for its dynamics to be regular? Finally, what does Nature need a chaotic neuron for? We will attempt to answer these questions by considering in detail a minimal neural network consisting of two coupled neurons only.

3.2 Regular and chaotic dynamics of two coupled neurons

For elucidation of the mechanisms of the phenomena observed, the model for a chaotic neuron must be "as simple as possible but not simpler".¶ We think that the Rose–Hindmarsh model (1.3) meets this requirement.

† In analysis of individual dynamics, the neuron is isolated from its neighbours either physically (removed from the ganglion) or chemically (the neurons connected to the one of interest are strongly hyperpolarised and, hence, exhibit no activity).

‡ The Lyapunov dimension is calculated as follows. The Lyapunov exponents are arranged in descending order $\lambda_1 \geqslant \lambda_2 \geqslant \ldots 0 \ldots \geqslant \lambda_n$. The amount of stable directions needed for compensation of stretching by contraction is taken into account. The attractor dimension D_λ determined in this fashion lies between m and $m+1$, where m is the number of the exponents in the sequence given above, whose sum is still positive but becomes negative on addition of λ_{m+1}. The fractional part d of dimension $D_\lambda = m + d$ $(d < 1)$ is found from the equality $\sum_{s=1}^{m} \lambda_s + \lambda_{m+1} d = 0$.

¶ These words of Einstein are known to refer to theory, but we think they are also true for models.

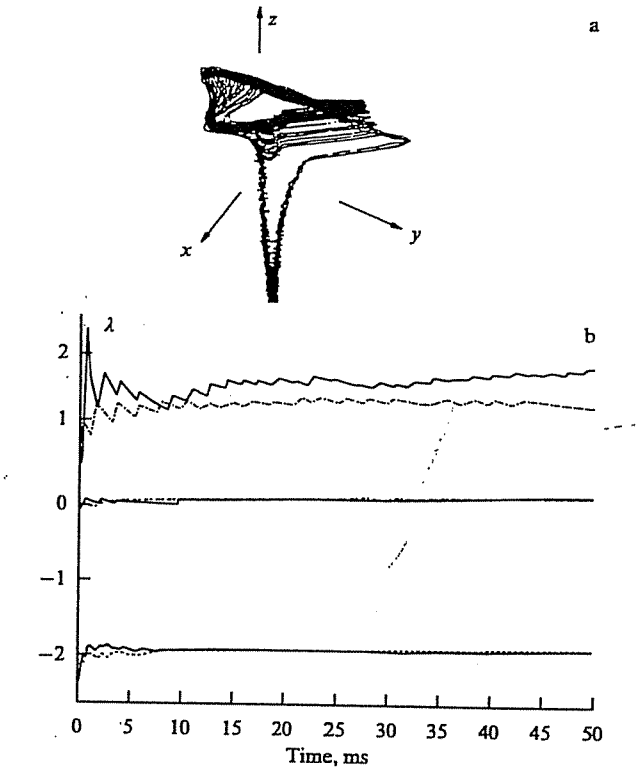

Figure 4. Features of deterministic chaos generated by the LP neuron [40]: (a) state space reconstruction from a long time series, this is a strange attractor; (b) the solid lines represent the Lyapunov exponents of an isolated LP neuron and the dotted lines represent the Lyapunov exponents of a LP neuron controlled by a inhibitory coupling from a PD neuron ($\lambda_1 > 0$; $\lambda_2 \approx 0$; $\lambda_3 = -2$).

3.2.1 Electrical coupling. We first address electrical coupling that is more familiar to physicists. Two electrically coupled chaotic neurons of the form (1.3) are described by the following equations ($b = 1$, $c = 1$) [17]:

$$\dot{x}_1 = y_1 + ax_1^2 - x_1^3 - r_1 + I - [\epsilon + \eta(t)](x_1 - x_2), \quad (3.1)$$

$$\dot{y}_1 = 1 - dx_1^2 - y_1, \qquad \dot{z}_1 = r[s(x_1 - x_0) - z_1],$$

$$\dot{x}_2 = y_1 + ax_2^2 - x_2^3 - r_2 + I - [\epsilon + \eta(t)](x_2 - x_1),$$

$$\dot{y}_2 = 1 - dx_2^2 - y_2, \qquad \dot{z}_2 = r[s(x_2 - x_0) - z_2]. \quad (3.2)$$

Here ϵ characterises the value of coupling that is interpreted as synapses conductance and $\eta(t)$ is a weak Gaussian noise with zero mean.

Electrically coupled chaotic oscillations received much attention in the last 10–15 years (see, e.g., Refs [7, 41, 42]). It is known, specifically, that such a system possesses an invariant manifold specified by the conditions $x_1(t) = x_2(t)$, $y_1(t) = y_2(t)$, and $z_1(t) = z_2(t)$. The neurons behave identically on such a three-dimensional manifold of the subsystem (the mismatch signal is zero). If this manifold is stable, then chaotic synchronisation is established in the system [7]. One can show that coupled Rose–Hindmarsh neurons (1.3) are also chaotically synchronised [17] at sufficiently strong coupling. Theoretical analysis is rather simple in this case. We consider a system of equations for the variables $u(t) = x_1(t) - x_2(t)$, $v(t) = y_1(t) - y_2(t)$, and

$w(t) = z_1(t) - z_2(t)$. By constructing the Lyapunov function

$$L(t) = \frac{V(t)^2}{2} + \frac{2au(t)^2}{b^2} + \frac{w(t)^2}{2rs},$$

we can readily verify that this system possesses a stable equilibrium state $(u, v, w) = (0, 0, 0)$, i.e. $dL/dt < 0$ when

$$\epsilon > \frac{1}{2} \max\left[-3x_1(t)x_2(t) - \left(\frac{b}{r} - a\right)\left(x_1(t) + x_2(t)\right) + \frac{b^2}{16}\right]. \tag{3.3}$$

Since $x_1(t)$ and $x_2(t)$ are limited, it follows from (3.3) that the electrically coupled Rose–Hindmarsh neurons are stochastically synchronised for sufficiently large ϵ.

This is also confirmed by numerical experiments. If we omit from consideration a small interval ϵ in the neighbourhood $\epsilon \approx 0.2$, where the neurons behave regularly (Figs 5a,b), then the neurons are not synchronised at weak coupling. For $\epsilon \leqslant 0.5$, the neurons are chaotically synchronised. It is 'intermittent synchronisation', i.e., it breaks every now and then (Fig. 5c). For strong coupling ($\epsilon \geqslant 0.5$), the neurons are completely chaotically synchronised (Fig. 5d). As an estimate for the extent of synchronisation in these model experiments we can use a mean root square of the distance between the time series produced by coupled neurons

$$D^2(\tau, \epsilon) = \frac{1}{N_s}\sum_{k=1}^{N_s}\left[x_1(k) - \xi x_2(k+\tau)\right]^2. \tag{3.4}$$

Here τ is the temporal shift providing the minimal value of D^2 and N_s is the total number of points in the time series. This estimate of the extent of synchronisation is convenient for description of the 'coordination' between pulsations with arbitrary phase shift relative to each other. The constant coefficient ξ is employed here to reduce the compared time series to one amplitude level. We emphasise that the effects described above that arise at electrical coupling of chaotic neurons are not specific for biology only. Similar phenomena were also observed in different electronic experiments (see, e.g., Refs [41, 42]).

3.2.2 Reciprocal inhibitory coupling. This type of coupling is, evidently, the most typical one in small neural networks, in particular, in CPGs (Fig. 6). The key role in coordinated behaviour and regularisation of dynamics of the coupled chaotic neurons belongs in this case to chemical synapses. In the context of modelling, it is essential that the coupling between the neurons occurring in this fashion is characterised by the presence of a threshold and a constant level of rest potential. Consequently, in the equation describing the membrane potential x_1 of a neuron we add a synaptic current associated with the action of another neuron (with potential x_2) of the form

$$-\left[\epsilon + \eta(t)\right]\left[x_1(t) + V_c\right]\Theta\left[x_2(t - \tau_c) - X\right]. \tag{3.5}$$

Here, as before, ϵ is the strength of the coupling and $\eta(t)$ is a small zero mean noise [17]. The thresholding of synaptic action is taken into account in the Heaviside function $\Theta(w)$, X is the threshold, V_c is the reverse potential, and τ_c is the synaptic delay associated with the chemical mechanism of transmission of excitation from presynaptic to postsynaptic membrane.

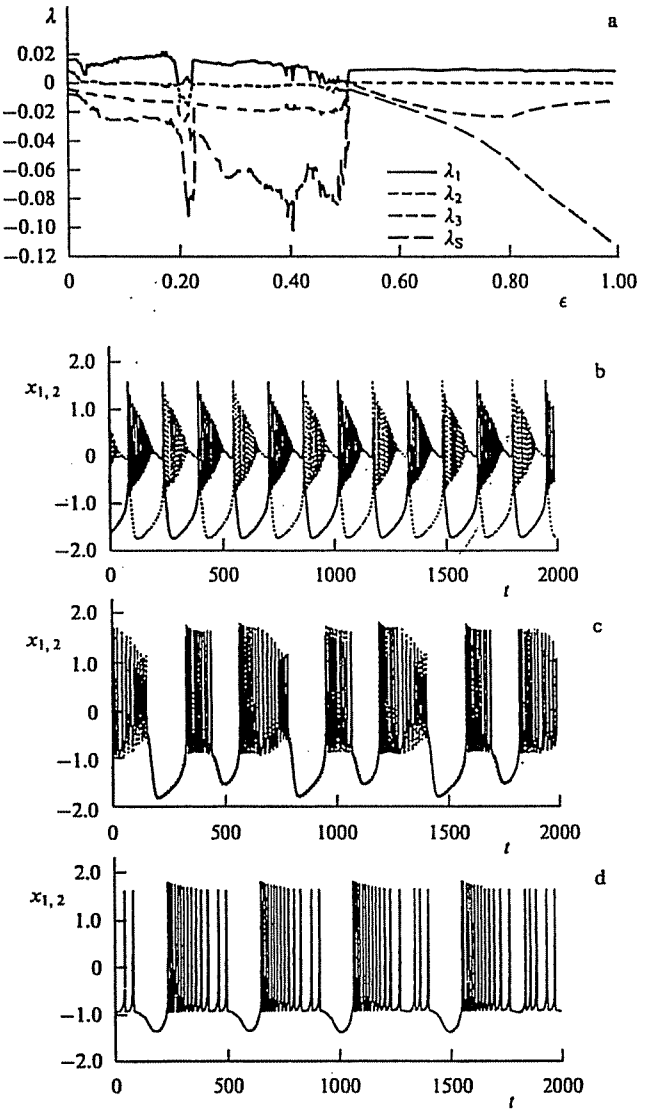

Figure 5. The membrane potentials of two x_1 (——) and x_2 (– – –) electrically coupled Rose–Hindmarsh models [17]: (a) the Lyapunov exponents depend on the value of the coupling ϵ; (b) out of phase synchronisation of neurons for small region of the coupling ($\epsilon \approx 0.20$); (c) intermittent stochastic synchronisation ($\epsilon < 0.5$); (d) complete stochastic synchronisation ($\epsilon > 0.5$).

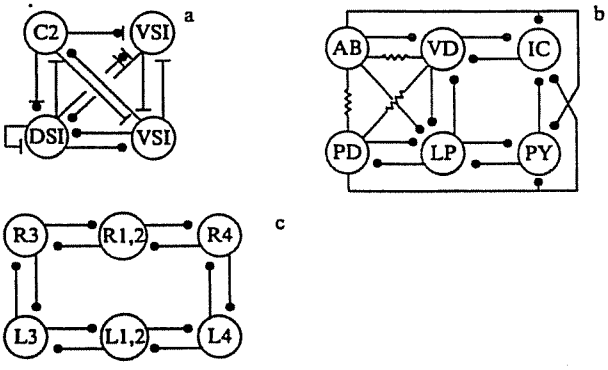

Figure 6. Chains of neurons forming the CPG for: (a) swimming CPG of a tritonia; (b) pyloric CPG of a lobster; (c) heart CPG of a medical leech. The black circles mean inhibitory coupling; T-shaped ends mean excitatory coupling, sign of resistors mean electrical coupling, and mixing coupling is represented by a combination of these symbols.

Consider a rather typical situation of double inhibitory coupling: from neuron 1 to neuron 2 and from neuron 2 to neuron 1. Note that such a reciprocal coupling is realised through two different synapses. The basic equations for such a neural network are written in the form

$$\begin{aligned}
\dot{x}_1 &= y_1 + ax_1^2 - x_1^3 - z_1 + I \\
&\quad - \left[\epsilon + \eta(t)\right](x_1 + V_c)\Theta\left[x_2(t-\tau_c) - X\right], \\
\dot{y}_1 &= 1 - dx_1^2 - y_1, \qquad \dot{z}_1 = r\left[s(x_1 - x_0) - z_1\right], \\
\dot{x}_2 &= y_2 + ax_2^2 - x_3^2 - z_2 + I \\
&\quad - \left[\epsilon + \eta(t)\right](x_2 + V_c)\Theta\left[x_1(t-\tau_c) - X\right], \\
\dot{y}_2 &= 1 - dx_2^2 - y_2, \qquad \dot{z}_2 = r\left[s(x_2 - x_0) - z_2\right]. \qquad (3.6)
\end{aligned}$$

Computer experiments for inhibitory coupling used $X = 0.85$, $V_c = 1.4$, and $x_0 = -1.6$. The experiments were performed at small τ_c, therefore the system (3.6) demonstrated only finite-dimensional behaviour.

Results of the experiments are shown in Fig. 7 and demonstrate two remarkable phenomena. First of all, synaptic coupling regularises the behaviour of individual chaotic neurons almost throughout the region of variation of controlled parameters ϵ, τ_c (except for a very weak coupling). It is, indeed, a remarkable fact. The coupling of two chaotic oscillators usually gives rise to complication of chaos (i.e., the increase of attractor dimension, the growth of the Kolmogorov–Sinai entropy, and so on). The degree of complexity remains at least the same as a result of chaotic synchronisation. Whereas in our case, the chaos transforms to order nearly in all the significant parameter region. The results indicate that this phenomenon is associated with the action of the synaptic coupling specified in (3.5). But it is only a model. Can this phenomenon be observed in experiments on living neurons? Results of processing of sufficiently long time series obtained from an isolated neuron-oscillator (LP neuron of a lobster [40]) and from the same neuron to which a chaotic signal is sent through chemical synapses from another neuron (PD, Fig. 6b) are presented in Fig. 4b and Fig. 8. It is clear that the chaotic action that is realised through inhibitory coupling regularises the behaviour of a living neuron significantly. This also follows from analysis of positive Lyapunov exponents (the positive exponent decreases by one and a half times in the case of a controlled neuron, see Fig. 4b) and from analysis of time spreading between the spikes and of the number of spikes in the burst (Fig. 8).

Another phenomenon that was observed in investigation of the system (3.6) is plasticity. As seen from Fig. 7, even a small variation of the parameters of synaptic coupling leads to bifurcations and to qualitative changes in the synchronisation of two inhibitorily coupled neurons. These may be total phase synchronisation of neurons, antiphase synchronisation, or synchronisation with a definite constant phase shift.

3.2.3 A little more about plasticity. We shall now briefly consider the results of the investigations of the dynamics of two chaotic Rose–Hindmarsh neurons at excitatory synaptic coupling and at mixed coupling (electrical plus inhibitory couplings) [17, 43].

The dynamics of a neural pair with reciprocal excitatory coupling may also be modelled by Eqns (3.6), with the only difference $V_c = 0$ that it is essential however. When $V_c > 0$, the signal transmitted through synapses hyperpolarises the

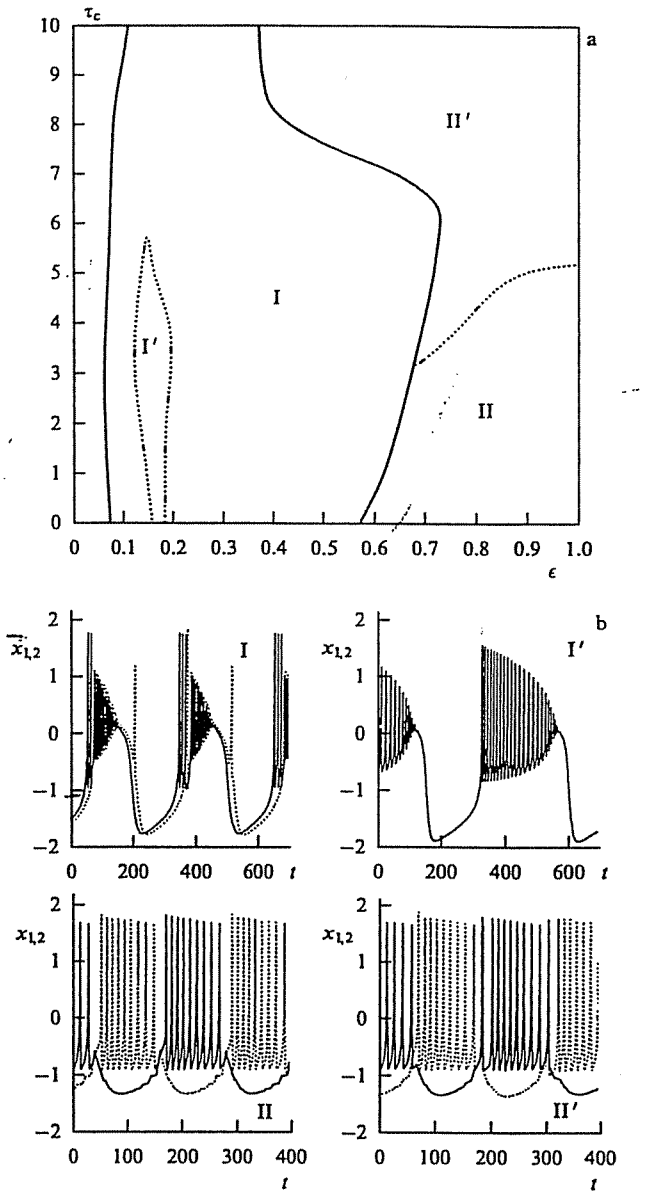

Figure 7. (a) Space of parameters 'synaptic time delay (τ_c) — value of the coupling (ϵ)' for two neurons with reciprocal inhibitory coupling. One can see four different types of synchronisation illustrated by plate (b). (b) Time series of oscillations x_1 (——) and x_2 (– – –) of two inhibitory coupled neurons corresponding to four different region of parameters in plate (a) τ_c, ϵ [17].

postsynaptic membrane, inhibiting its activity. For $V_c \leqslant 0$ the membrane is depolarised and the probability of pulse generation increases. That is why the latter coupling is called excitatory. Results of the analysis of the system (3.6) for $V_c = 0$ are given in Fig. 9. Three types of synchronous activity were observed. They differ by the number of spikes in the bursts, by their duration between the spikes, and by oscillatory amplitude. Can the diversity of synchronisation regimes be used to control, for example, the frequency of slow pulsations of the synchronised neurons? Below we present an example that demonstrates a fascinating regularity of the transitions from slower to faster pulsations as the value of inhibitory coupling is decreased.

We now address a neural pair with mixed coupling: reciprocally inhibitory and electrical. Such a minimal neural

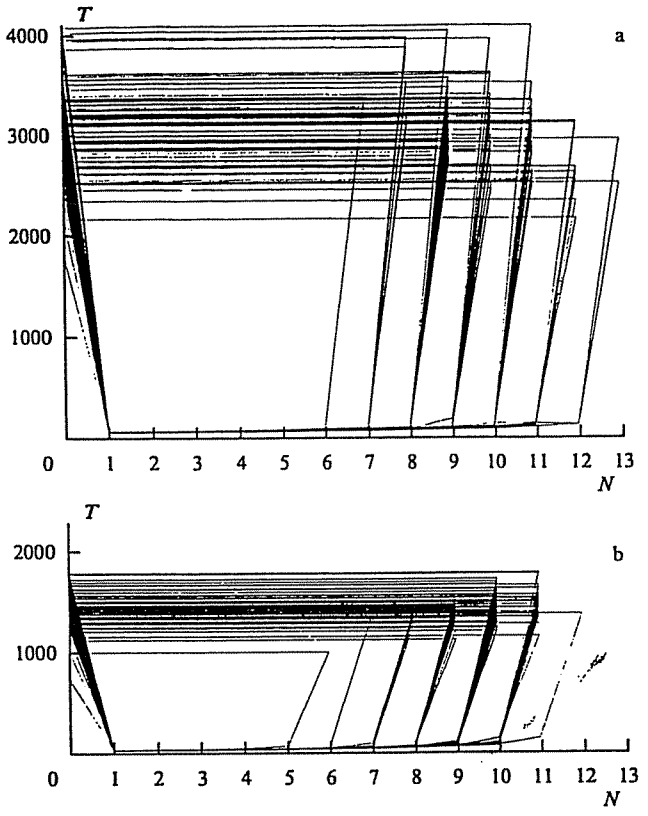

Figure 8. Regularisation of a LP neuron dynamics through an inhibitory action of a PD neuron [40]: (a) Spread in the spike number N and inter-spike intervals T for an isolated LP neuron; (b) the same for the LP neuron controlled by the PD neuron. One can see only one burst of 6 spikes or two bursts of 12 spikes along the time series in the case (a). The maximal number of bursts contains 8 or 9 spikes. The inter-spike intervals spread from 2000 to 4000 units of time. The spread in inter-spike intervals is much smaller for the controlled neuron.

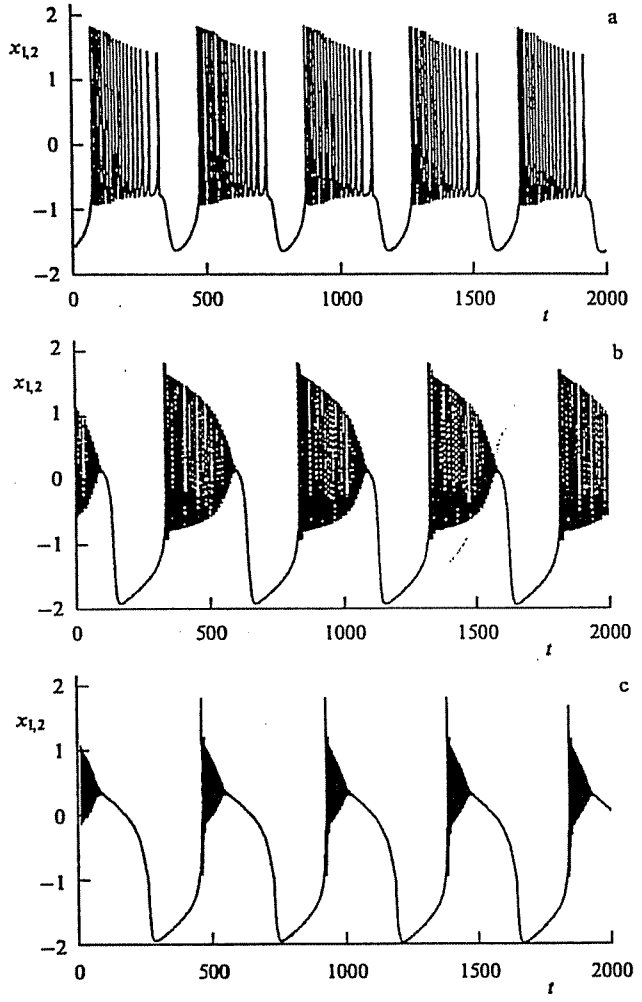

Figure 9. The membrane potentials x_1 (——) and x_2 (– – –) for two reciprocal excitatory coupled Rose–Hindmarsh models — the synaptic time delay is $\tau_c = 4$. The synchronisation leads to periodic motion: (a) $0.05 \leqslant \epsilon < 0.1$; (b) $0.1 \leqslant \epsilon < 0.15$; (c) $0.15 \leqslant \epsilon < 1$ [17].

network is described by Eqns (3.6) the right-hand sides of which (or, more exactly, the equations for membrane potentials x_1 and x_2) are supplemented by synaptic current from electrical synapses as in Eqns (3.1). Analysis of the dynamics of this model is summed in Fig. 10, where the period of slow oscillations of synchronised neurons is plotted versus inhibitory coupling ϵ_i for fixed electrical coupling $\epsilon_e = 0.1$ [43]. A remarkable phenomenon is observed: the period of pulsations increases in a regular fashion as ϵ_i is increased, showing a dependence of the form of a staircase. The steps correspond to regions of stable pulse generation with a fixed number of spikes. Each new step corresponds to the change of the number of spikes in the burst by unity. The value of inhibitory coupling is known to depend on the concentration of different chemical substances. Thus, the model gives a hint how to regularly control the CPG period by choosing a concentration of the neuromediator controlling the parameter ϵ_i.

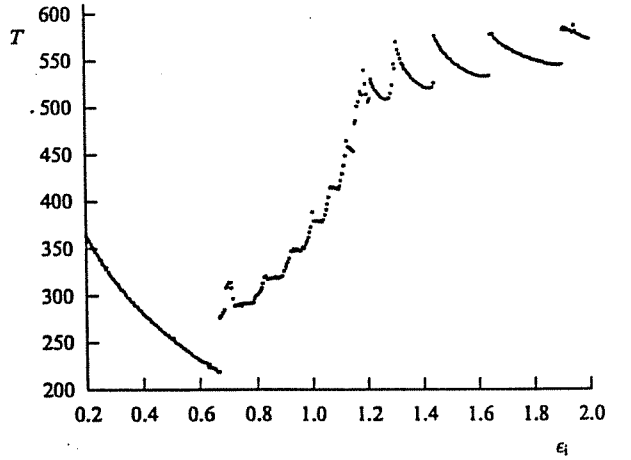

Figure 10. Dependence of the burst period in minimal nerve system (two Rose–Hindmarsh neurons with mixed coupling) on the value of inhibitory coupling ϵ_i at constant electrical coupling $\epsilon_e = 0.1$ and $\tau_c = 4$ [43].

4. Rhythmic activity of small neural networks

A neural network is organised so that it is capable of providing the necessary rhythm of muscular activity even when there is no feedback signal from the muscles. It was already noted that a CPG generates a signal that contracts the

muscles used in the rhythmic movements with the required phase (the historical background and references to early works can be found in the review [44]). A CPG may also operate independent of the brain. Animals may produce complex patterns of behaviour even on decerebration [45]. For instance, decerebrated cats may mate. For the construction of a CPG theory we should address three key points: the oscillatory models of a neuron (or a group of neurons) that should be used for description of the operation of an autonomous CPG; their interaction; and the fashion in which the information from sensors and cerebrum are used by CPG.

These problems have been clarified significantly for lower animals, for instance, lobsters. Detailed experiments [34] on the CPGs of pylorical and other stomatogastric rhythms of a lobster furnished much information about their organisation. All the neurons belonging to them were identified and it is understood how they communicate with each other. For example, a pyloric CPG consists of 14 neurons combined into 6 functional groups: LP and PY neurons (Fig. 6b) control contracting muscles, VD and PD neurons govern stretching muscles, IC neuron determines an auxiliary rhythm, while AB interneuron is a pacemaker for the operation of the CPG and is not connected with muscles.

Such a detailed knowledge of the basic scheme allows for the construction of a complete dynamical theory of autonomous stomatogastric CPG of a lobster (see Ref. [34]).

4.1 Space-time symmetry and segmentation. Examples

Even when we speak solely about mechanical movements, we should bear in mind that a great amount of neurons control them. Consider as an example a locust. Its flight is a complicated process involving coordinated movements of nearly all organs. There are at least five types of rhythmic activity concerned with aerodynamic effects only [46]: asymmetric alteration of wing beat amplitude, asymmetric alteration of the angle of attack of the wings, phase shift of the wings within the wing beat cycle, bending the thorax, ruddering of the hind legs. The locust performs these movements in different combinations and uses about 10% of the neurons of its central neural network [46]. However, even in this difficult case analysis of controlling processes is not hopeless. The point is that most of the muscles controlling the flight are segmental homologues, as are the corresponding motor neurons and CPGs. Consequently, different types of mechanical motions follow the same basic principles of rhythm realisation [46].

The second significant aspect is that all the vital movements possess a pronounced space-time symmetry. Different types of symmetries may correspond to different speeds, as in the case of animals that produce locomotion with their legs. On the other hand, the space-time symmetry may remain almost unchanged for an entire range of speeds, for example in the case of the fishes which swim by means of the travelling wave that sweeps along their body. An attempt to formalise intuitive concepts about coordinated and synchronised locomotion encounter many difficulties. Indeed, for similar types of oscillations that differ only by a time shift, the latter can be chosen as a measure of phase shift. For nonidentical oscillations, the phase difference is as undetermined as the phase itself, although we can speak about mean synchronisation [7, 17] (see also Section 3). It is possible to choose a reasonable start even for such oscillations having different time patterns. For instance [47], if all the animal's extremities contact the surface only once per period of locomotion, then the instant of this contact may be chosen as the origin of the phase. This already enables one to give a qualitative description of space-time symmetry. Figure 11 gives a schematic representation of the paces typical of four-leg animals' locomotion. Figure 12 displays some of them using an example of the animal of the authors' preference.

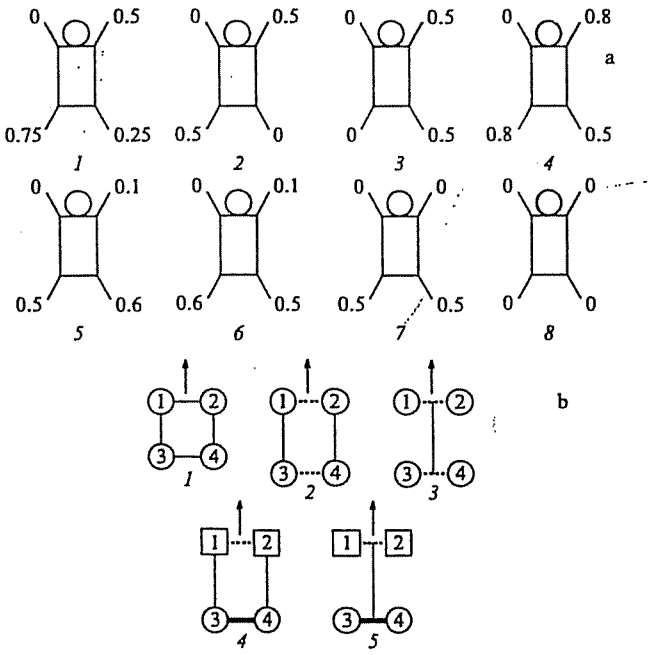

Figure 11. (a) Phase relationships between limbs: *1* — step; *2* — trop; *3* — amble; *4* — slow gallop; *5–6* — different types of fast gallops; *7–8* — different types of jumps. (b) Sketch of coupled oscillators with five different symmetries. The symbols ○ and □ depict two different types of oscillators, the lines ——, ···, ═══ represent three types of coupling [47].

Unfortunately, the mechanisms of CPG operation in higher vertebrates are not completely clear in spite of joint efforts by experimentalists and theoreticians. Let us now address less exciting but more advanced investigations of the animals that have pronounced segmented structure and simple space symmetry. The general neural organisation of locomotion in vertebrates is very conservative both to interspecific changes and evolution. Consequently, lower vertebrates may be regarded as models of higher species.

Locomotion of the animals with segmented structure of neuromuscular system (fishes, worms, crustacea, and the like) consists of repeated sequences of similar coordinated movements of different segments. Such a movement for fishes is a form of a travelling wave propagating along the body at a constant speed. The waves conserve their features even when the speed of swimming is changed, so that the wave number ranging from 0.6 to 1.0 [48] is constant along the body length of the swimming animal. The speed is controlled by the frequency and is approximately proportional to it (Fig. 13). Naturally, the range of speeds and frequencies depends on the type and size of fish. For example, for trout the frequencies range from 3 Hz to 25 Hz. Variations of the amplitude of movements are pronounced only at small speeds when it decreases (Fig. 13) [48, 49]. Such a motor picture is not a

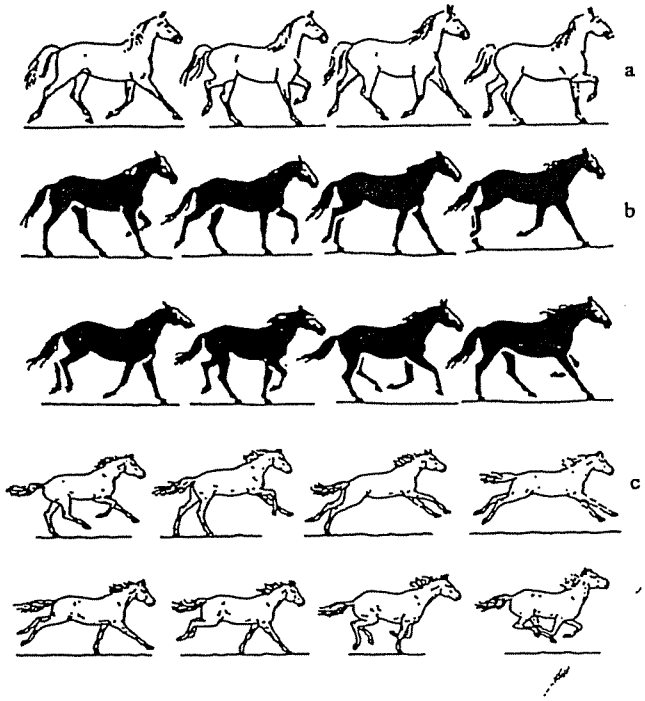

Figure 12. Trop (a), slow gallop (b) and fast gallop (c) [47].

passively propagating wave. It arises as a result of contraction of the muscles controlled by coordinated motor neurons. As the fish moves forwards, these contractions occur from segment to segment with a nearly constant phase shift, and do not depend on frequency. This assures constant wavelength and propagation velocity along the body.

The phase ratios between the segments were first described for a dogfish shark [50], and later for eel, trout, dace [48], lamprey [51, 52], and frog larvae [53]. The fishes have a minimal delay of 1–2% per each segment during swimming without change of direction, although this value may vary and even be negative, thus providing swimming backwards [50].

Observation of evolution of the animals at early stages and comparison of the changes in their neural networks and space-time symmetries show how learning proceeds. For example, the earliest stage of frog larvae development is the stage of irregular movements which is then replaced by the stage when the muscles along one side of the body are contracted simultaneously to form a C-shaped bending that turns in different directions alternately. At a later stage, movements of this type are transformed to a travelling wave (for fishes) or to a standing wave (for salamanders, Fig. 14). A lamprey, like frog larvae, learns to swim in an optimal fashion by replacing a standing wave by a travelling wave at maturity.

4.2 The mechanisms of intersegmental coordination

The mechanisms that may be used to explain the emergence of unidirectional waves with constant intersegmental phase shift include, among others, a gradient mechanism, a mechanism of 'slave' oscillator, and a mechanism of nonreciprocal couplings.

4.2.1 Gradient mechanism. Consider, as an example, the swimming system of a lobster. It was hypothesised that the phase shift between the flaps of the fins is a result of a smooth dependence of natural frequencies of neural centres on coordinate along the body [54]. A natural model for the

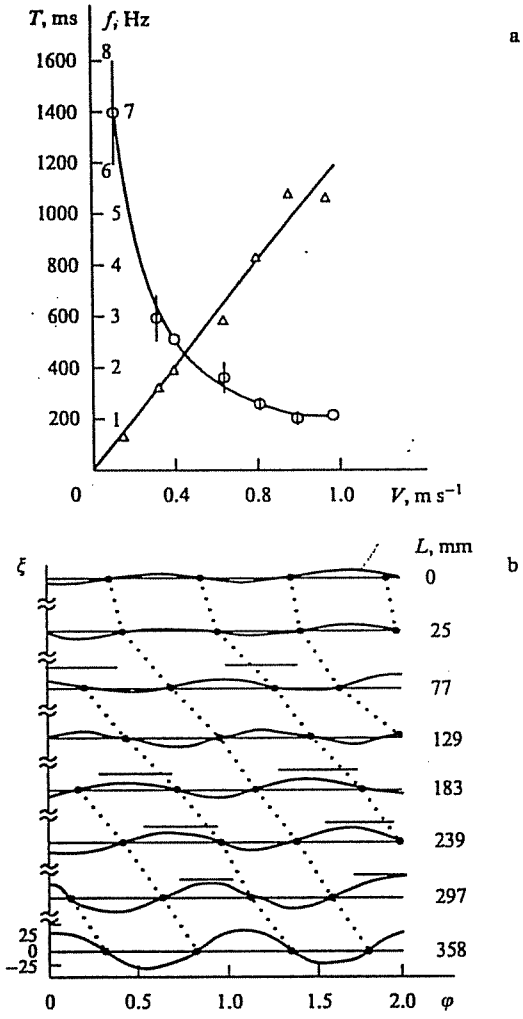

Figure 13. (a) Frequency f (△) and period T (○) of lateral displacement of the animal V. (b) Phase (φ) of lateral displacement of the body V for different distances to the head L [48, 49].

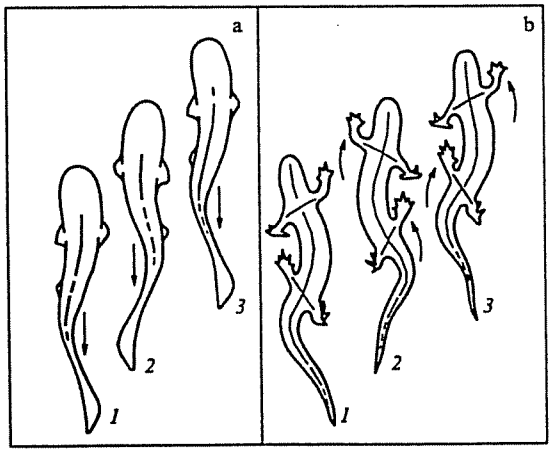

Figure 14. Wave motion of the animal — travelling wave along the body of the shark (a) and standing wave along the body of the salamander (b).

CPG realising such a mechanism is a chain of coupled oscillators [55]. Such a model also allows for the fact that rhythmic activity is conserved in small isolated portions of the spinal cord (e.g., in 1–5 segments of a lamprey [49]). It is

essential that the rhythm generated by such a chain is autonomous. The rhythm parameters in experiments change only slightly under the action of external forces and are rapidly restored when these forces are eliminated. In particular, fictive swimming of a lamprey disturbed by forcing is restored in a few periods [56, 57], which is inherent in oscillators with a strongly attracting limit cycle (see, e.g., [58]).

Analysis of the model in the form of a chain of phase oscillators demonstrated [59] that the phase shift along the chain is not constant, although a travelling wave is formed in such a system. However, the gradient (of frequencies) observed along the spinal cord makes us take this mechanism into account even when it is not primary.

4.2.2 Slave oscillators. In the frames of a model for a slave oscillator, a travelling wave is formed if at least one oscillator has a frequency higher than the remaining portion of a uniform chain (Fig. 15). This master oscillator initiates the one following it (slave oscillator) with a definite phase shift, and so on. Apparently, the phase shift will be constant for the remaining portion of the uniform chain of segments. This model for a spinal CPG is especially attractive in that different regimes of swimming are readily realised in it, especially switching over from swimming forwards to swimming backwards, for which it suffices to increase the level of excitation of one neuron-oscillator. The hypothesis of slave oscillator [60] is also confirmed by experiments on isolated spinal cord of the lamprey. The key points of these experiments are as follows [46]. Each segment may be made the master one by increasing the level of excitation (and, consequently, frequency). The influence of the master segment is distributed along the spinal cord and is retained after it is divided into portions, each portion being capable of demonstrating fictive swimming forwards and backwards at appropriate local forcing. The phase shift at local forcing is the same for all segments until their excitation level is uniform and smaller than that of the master segment. These observations agree rather well with analysis of a CPG model [61]. The segments are synchronised if their excitation levels are identical. If the excitation level of one of the segments is 1–5% higher, this segment becomes the master one, independent of its position in the chain. All the other oscillators are slave ones and have a constant phase shift between them in both directions from the master segment. Results of modelling according to which the higher the excitation levels of master and slave oscillators, the larger the phase lag, also agree with experiments. For a given difference of excitations between the master and slave segments, the phase shift does not depend on the excitation level and, hence, on frequency. In other words, the wavelength of the travelling wave along the lamprey body will be constant irrespective of the speed of swimming.

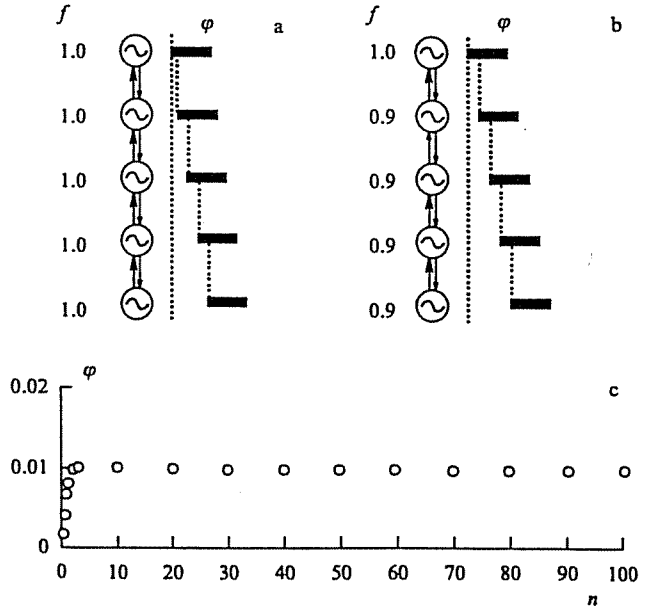

Figure 15. Phase lag in a chain of oscillators (φ): (a) with equal frequencies ($f = 1$) and non-reciprocal coupling; (b) with reciprocal coupling and master oscillator of higher frequency; (c) the dependence of the phase lag (φ) on the number of oscillators along the chain n [55].

4.2.3 Intersegmental coupling. The two mechanisms discussed above are based on the effect of the intrinsic parameters of segmental oscillators on intersegmental phase shift. However, the phenomena observed in some experiments cannot be reduced to these two mechanisms. Let us consider, for instance, a leech in which oscillations of an isolated segment of the spinal cord have some peculiarities as compared to their behaviour on the whole. This makes us to reject the supposition that the intersegmental coupling is weak [62–64]. These characteristic features are: excitation of oscillations in a single element is hindered and needs strong stimulation; the episodes of fictive swimming are very short (of about several seconds as a rule) in a completely isolated centre; the phase relationships between isolated cells inside segments differ from those in the segments which are part of long chains; the oscillations of the membrane potential of an isolated segment are strongly deformed in shape as compared to the natural one.

These facts indicate that, although a neural network generating swimming movements of a leech may be regarded as consisting of individual segments, the coupling between them is strong. Besides, the couplings between the segments are not local, they extend to remote segments too. Experiments aiming at determining the range of couplings employed sample blocking of couplings or blocking of oscillations of neural centres, when intersegmental pulses could propagate through remote couplings escaping the blocked portion. Both the ends of the chain remained synchronised even when five segments were blocked, which indicates that the couplings are indeed global [64].

The three mechanisms described above do not contradict each other, in principle, and may be realised in different combinations.

4.2.4 Sensory feedback. The intersegmental coordination analyzed above does not take into account the effect of the feedback that transports information from sensor neurons to CPGs. Sometimes these effects are significant. For example, such a feedback is, evidently, the cause for different phase shifts of a swimming leech and of the spinal cord at fictive swimming (12° and 8° per segment, respectively) [64]. Such an influence of sensory feedback is also manifested by the behaviour of animals in extraordinary situations. For instance, a dogfish shark whose nerve cord has been severed behind the head and which has been deafferented along more than half the length of its body will swim for hours without any stimulation. Its autonomous rhythmic activity is also

confirmed by the fact that the parts of the body separated by the region of deafferentiation are well coordinated even when the animal is rendered motionless by injection of curare that paralyzes the muscles [65]. On the other hand, the sensory feedback affects the rhythm and amplitude of swimming CPG. If the tail of the paralysed shark is forced to oscillate with a frequency different from that of autonomous CPG rhythm, then the signals from the CPG will have the frequency of external forcing (!) [66].

Other examples of sensory feedback leading to CPG synchronisation, are also available. In this case, both ideal one-to-one synchronisation and intermittent synchronisation (when the periods of CPG output and sensor input coincide only part of the time) are possible, if the periods are close. Let us consider some examples of extreme influence of sensory feedback that may be useful for testing the adequacy of the models proposed. Intriguing cases of fictive swimming of an isolated spinal cord of lamprey were described in Ref. [59]. On injury of the spinal cord, its portions above and below the injured spot were synchronised at 2 : 1. Analogous effects were observed for animals with four limbs. A swimming turtle usually chooses a pattern of movements similar to land animals: the diagonal legs move in phase and two diagonal pairs are phase shifted by half a period relative to each other. In definite laboratory conditions, the front leg of the turtle may move at a double frequency relative to the hind leg on the same side of the body [67].

Still another series of investigations is concerned with the use of a treadmill [67–70]. It was shown in Ref. [68] that locomotion (walking and running along a moving band) of decerebrated cats was controlled by electric stimulation. As the stimulation was increased, the cats could change their pace from trot to gallop. These investigations were modified by using a split-belt treadmill, each belt moving at its own speed. Until the speeds differed by no more than 2–3 times, a 1 : 1 synchronisation of hind legs was observed. But when the difference amounted to 4–6 times, the 2 : 1 synchronisation became stable. This phenomenon was analysed in Ref. [71] on an example of five possible variants of four model coupled oscillators (Fig. 11b). Theoretical group analysis verified that systems *1* and *3*, actually, allow for bifurcations of symmetry breaking as a result of which a 2 : 1 synchronisation occurs between different subsystems.

In conclusion we can say that a motor system consists of a neural control network, extremities and/or body with muscles, and sensory feedback. In the case of repeated or stereotype behaviour, CPG controls rhythmic activity even in the absence of sensory feedback. Real behaviour is a product of joint action of a neurophysiological system, in which the CPG transmits the signal to the muscles through motor neurons and the axons of the sensor neurons transport the sensor information back to the neural network. The motor neurons are output (passive) elements of the CPG and do not take part in rhythm formation. The periodic oscillations generated by neurons from different segments may be partially or completely synchronised, depending on external conditions.

4.3 Phase description. General idea

The phase description of weakly coupled oscillators is well known [72] and is broadly employed for construction of different models, including CPG models. It is based on a supposition which merely means that oscillators demonstrate stable periodic motion even in the absence of coupling, while interaction leads to small deviations from this periodic behaviour (limit cycle in phase space). The fundamental features of phase models may be explained as follows [72, 73]. A limit cycle corresponds to stable periodic motion, and its state is completely determined by the phase φ, i.e., by the coordinate mapping the points on this cycle. On choosing the appropriate time scale, the equation $\mathrm{d}\mathbf{x}/\mathrm{d}t = \mathbf{F}(\mathbf{x})$ for periodic motion $\mathbf{x}(\varphi) = \mathbf{x}(\varphi + 2\pi)$ may be represented in the form

$$\mathbf{x} = \mathbf{x}_0(\varphi), \qquad \frac{\mathrm{d}\varphi}{\mathrm{d}t} = \omega, \tag{4.1}$$

where $\mathbf{x} = \mathbf{x}_0(\varphi)$ is the orbit of limit cycle specified parametrically. The phase introduced in this fashion may be generalised to the trajectories close to the given limit cycle. To this end a thin tube is chosen in the neighbourhood of the limit cycle and its scalar field $\varphi(x)$ is determined such that

$$\frac{\mathrm{d}\varphi}{\mathrm{d}t} = \mathrm{grad}_{\mathbf{x}}\, \varphi \mathbf{F}(\mathbf{x}) = \omega. \tag{4.2}$$

For a perturbed system

$$\frac{\mathrm{d}\mathbf{x}}{\mathrm{d}t} = \mathbf{F}(\mathbf{x}) + \epsilon \mathbf{p}(\mathbf{x}, t) \tag{4.3}$$

we have

$$\frac{\mathrm{d}\varphi}{\mathrm{d}t} = \mathrm{grad}_{\mathbf{x}}\, \varphi\left[\mathbf{F}(\mathbf{x}) + \epsilon \mathbf{p}(\mathbf{x}, t)\right] = \omega + \epsilon z(\varphi)\, \mathbf{p}(\mathbf{x}, t),$$

or, to the terms $\propto \epsilon^2$,

$$\frac{\mathrm{d}\varphi}{\mathrm{d}t} = \omega + \epsilon z(\varphi)\, \mathbf{p}\left(\mathbf{x}_0(\varphi), t\right), \tag{4.4}$$

where the functions periodic over φ stand in the right-hand side. If the perturbation $\mathbf{p} = \sum_j V_{ij}(\mathbf{x}_i, t_i)$ is caused by interaction with the oscillators having similar features ($\omega_j = \omega_0 + 2\delta\omega_i$, where $\delta\omega_i \ll \omega_0$), then to the same approximation we have

$$\frac{\mathrm{d}\varphi_i}{\mathrm{d}t} = \omega_i + \epsilon \sum_{\substack{j=1 \\ j \neq i}}^{N} \left[\mathbf{z}_i(\varphi_i)\, \mathbf{V}_{ij}(\varphi_i, \varphi_j)\right], \tag{4.5}$$

where $V_{ij}(\varphi_i, \varphi_j) = V_{ij}\left(x_i(\varphi_i), x_j(\varphi_j)\right)$ are the functions periodic over φ_i.

Obviously, the phase perturbations $\psi_i = \varphi_i - \omega t$ will be slow ($\propto \epsilon$):

$$\frac{\mathrm{d}\psi_i}{\mathrm{d}t} = \epsilon \sum_{\substack{j=1 \\ j \neq i}}^{N} \left[\mathbf{z}_i(\psi_i + \omega t)\, V_{ij}(\omega t + \psi_i; \omega t + \psi_j) + \delta\omega_i\right].$$

Then, averaging over period $T = 2\pi/\omega$ gives

$$\frac{\mathrm{d}\psi_i}{\mathrm{d}t} = \sum_{j=1}^{N} H_{ij}(\psi_i - \psi_j) + \epsilon\delta\omega_i, \tag{4.6}$$

where

$$H_{ij}(\psi_i - \psi_j) = \epsilon \frac{1}{2\pi} \int_0^{2\pi} Z(\xi + \psi_i)\, V_{ij}(\xi + \psi_i; \xi + \psi_j)\, \mathrm{d}\xi. \tag{4.7}$$

Coming back to the original total phases $\varphi_i = \psi_i + \omega t$ we find the sought equations

$$\frac{d\varphi_i}{dt} = \omega_i + \sum_{\substack{j=1 \\ j\neq i}}^{N} H_{ij}(\varphi_i - \varphi_j). \tag{4.8}$$

Methods for calculation of the functions $H_{ij}(\xi)$ were described in Ref. [21]. In particular, for coupled Van der Pol equations

$$\ddot{x}_i + \delta(x_i^2 - 1)\dot{x}_i + (1 + \delta\omega_i)x_i = \left[\epsilon_1(\dot{x}_{i+1} - 2\dot{x}_i + \dot{x}_{i-1}) + \epsilon_2(x_{i+1} - 2x_i + x_{i-1}) + \epsilon_3(\ddot{x}_{i+1} - 2\ddot{x}_i + \ddot{x}_{i-1})\right] \tag{4.9}$$

the function of coupling is

$$H(\bar{\varphi}_i) = \epsilon_1 \sin\bar{\varphi}_i - (\epsilon_2 - \epsilon_3)(\cos\bar{\varphi}_i - 1),$$
$$\bar{\varphi}_i = \varphi_{i+1} - \varphi_i. \tag{4.10}$$

Consider an example of how these equations may be used.

4.4 A chain of identical oscillators: model for a swimming CPG of lamprey

A model system for controlling intersegmental synchronisation must take into account principal dynamical mechanisms and, of course, fit the available neurophysiological data.

Consider a swimming CPG of a lamprey. We represent the CPG as a chain of n identical oscillators and take into consideration only couplings with the nearest neighbours [74, 75]:

$$\frac{d\varphi_1}{dt} = \omega + H^+(\bar{\varphi}_1),$$
$$\frac{d\varphi_k}{dt} = \omega + H^+(\bar{\varphi}_k) + H^-(-\bar{\varphi}_k), \quad 1 < k < n, \tag{4.11}$$
$$\frac{d\varphi_n}{dt} = \omega + H^-(-\bar{\varphi}_{n-1}),$$

where $H^-(-\bar{\varphi})$ and $H^+(\bar{\varphi})$ are the functions describing the action on the oscillator of the neighbours preceding (descending action) and following it (ascending action). From the conditions of experimentally observed stable synchronisation with a constant phase shift along the chain two limitations are imposed on the functions $H^+(\bar{\varphi})$ and $H^-(-\bar{\varphi})$ [75]: (1) There exists a finite interval of values for $\bar{\varphi}$ on which $H^+(\bar{\varphi})$ and $H^-(-\bar{\varphi})$ are, respectively, monotonically increasing or decreasing functions that vanish at some points $\bar{\varphi}_R$ and $\bar{\varphi}_L$ inside this interval ($H^+(\bar{\varphi}_R) = 0$; $H^-(-\bar{\varphi}_L) = 0$); (2) At least one of the inequalities: $f'_{\bar{\varphi}}(\bar{\varphi}_L) < 0$ or $f'_{\bar{\varphi}}(\bar{\varphi}_R) > 0$ is fulfilled for the function $f(\bar{\varphi}) = [H^+(\bar{\varphi}) + H^-(-\bar{\varphi})]/2$.

When the above conditions are fulfilled (see Fig. 16), the system (4.11) is stably synchronised $d\varphi_i/dt = \Omega$ with intersegmental shift $\bar{\varphi}_k$ that is approximately equal for all k, except the near vicinities at the ends of the chain (Fig. 15). This shift is equal to $\bar{\varphi}_L$ or $\bar{\varphi}_R$, depending on the dominating interaction: the ascending $|H^+(\bar{\varphi}_L)| > |H^-(-\bar{\varphi}_R)|$ or the descending one $|H^-(-\bar{\varphi}_R)| > |H^+(+\bar{\varphi}_L)|$. The synchronisation frequencies are, respectively, $\Omega = \omega + H^-(-\bar{\varphi}_R)$ or $\Omega = \omega + H^+(\bar{\varphi}_L)$. In a noncrude case $|H^-(-\bar{\varphi}_R)| = |H^+(\bar{\varphi}_L)|$, the dependence

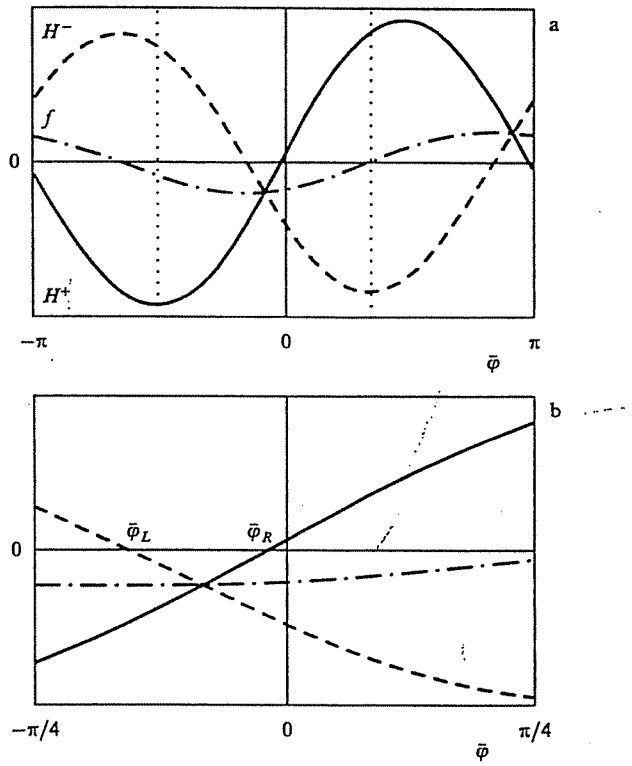

Figure 16. Example of the functions $H^+(\bar{\varphi})$ and $H^-(-\bar{\varphi})$, which satisfy the conditions discussed in the text: ——— $H^+(\bar{\varphi})$; – – – – $H^-(-\bar{\varphi})$; – · – f.

$\bar{\varphi}_k$ is determined by details of couplings and possible small spread of intrinsic frequencies.

Comparison of the model and results of experiments on controlling fictive swimming of lamprey shows that the ascending couplings dominate. Due to a varying value of ascending couplings, the model (4.11) makes it possible to choose the intersegmetal shift so that only one wavelength, indeed, exists along the chain. However, there is no mechanism to provide such a choice of coupling in this model. Perhaps, the key role in organisation of a needed phase shift belongs to remote intersegmental couplings [57, 76–78].

5. Synchronisation of neurons in the cortex

5.1 Possible role of synchronisation in information processes

Recent experimental investigations indicate that oscillations and related synchronisation processes may play a significant role in the brain, primarily, in perception and information processing. Here we speak only about processing of the oscillograms generated by individual neurons or spatially localised groups of neurons rather than about the averaged oscillatory activity of the brain that is usually associated with analysis of electroencephalograms (see, e.g., Ref. [79]).

The intrinsic oscillatory activity of localised portions of the cortex may be caused either by the activity of individual neurons or by the interaction of nonoscillating neurons forming a pair due to inhibitory or excitatory couplings. The Wilson–Cowan model (1.4) is an example of a model which

describes pulsations of such a pair. This model is used as an elementary unit for a large number of more complex dynamical systems which allow for a better understanding of the potentialities of synchronisation processes in the cortex [80].

It should be emphasised that neurons and neural ensembles in the cortex may be active in a rather broad frequency range, but a typical interval is from 10 to 50 Hz. It is a very low frequency in terms of computer engineering: the operating frequency is by six (!) orders of magnitude higher in modern computers. Why does the brain act much faster in non-arithmetic operations such as vision and recognition of objects? What ideas are realised by Nature in this unique neurocomputer?

There are no answers to these questions yet. The available concepts are primarily based on analogous parallel processing of signals and self-education. Experiments show that the necessary information is contained not only in the frequency but also in the phase of pulsations of neurons and neural assemblies (groups). Evidently, the phase synchronisation plays the most significant role in processes of perception and, particularly, visual image processing.

5.2 Vision: segmentation and binding problems

The principal feature of perception is the ability of the brain (its system of vision, in particular) to disintegrate the elements of a perceived picture (or scene) into 'coherent clusters'. This allows for coding different objects and even their features and for their subsequent recognition. Disintegration of images is referred to as segmentation or organisation of perception. Whereas unification of individual features into an integral image or of separate elements into a complete picture is called binding. The segmentation may be peripheral and central. Peripheral segmentation is based on the correlation of the qualitative characteristics of scenes (pictures, images) at the stage of perception. The central segmentation is based on a priori (associated with memory) knowledge about the visual scene.

How does segmentation occur in the brain? This question is not answered yet. Here we will consider a hypothesis that is based on the models which use results of recent biological experiments on an anaesthetised cat brain.

One of the most popular hypotheses today originates from the experiments on observation of stimulus-evoked oscillatory activity of the nervous cells responsible for perception. This hypothesis uses von der Malsburg's idea [81, 82] according to which the object initiates oscillatory activity of the neurons that code different properties of the object and are located in the corresponding portions of the visual cortex. One possible way of solving the problem of segmentation and binding is synchronisation of neuron activities which are spread over different portions of the cortex while they process features of the same object. Different objects are represented by different groups of neurons with nonsynchronous oscillations [83, 84].

Experiments verified that on stimulation of different portions of the retina, the groups of neurons in the primary visual cortex that are responsible for these portions were excited and had an oscillatory activity with the frequency of about 50 Hz. The oscillations of the neurons were synchronous inside each group [85, 86]. Synchronous oscillations of space-separated groups of neurons in the cortex were observed in two cases, either at identical stimulation of the relevant portions of retina or when the receptor fields of the neural groups space-separated in the cortex overlapped, i.e. were excited as a result of stimulation of the same portion of the retina [87, 88]. No synchronisation occurred between the excited columns of neurons when non-overlapping receptor fields were stimulated by different objects (e.g., by light bars moving in different directions) [89].

Experiments show that the groups of neurons in the primary visual cortex (columns) responsible for the same portion of the retina have different orientation preferences, i.e., they are responsible for different directions of motion of the stimulating object [90]. Experiments on stimulating one portion of the retina by several objects (light bars) moving in different directions (i.e., intersecting the field of vision at different angles) demonstrate that a particular group of synchronously oscillating neurons corresponds to each object. These groups are not synchronised [87, 91]. When a portion of the retina is stimulated by one moving object all the groups of neurons responsible for this portion oscillate synchronously. However, there is a constant phase shift proportional to the difference in the orientation preferences of different groups [92].

Emergence of synchronous activity of the groups of neurons corresponding to different neighbouring portions of a cat's retina was confirmed in Refs [85, 93, 94]. Besides, synchronisation of different areas of the cortex was revealed. Synchronisation of space-separated neurons inside a striate cortex was also demonstrated in experiments on a monkey's visual system [95, 96]. Later, experiments on cats showed that phase synchronisation may occur between the groups of neurons located in striate cortex and extrastriate cortex [97] and even between the columns of different cerebral hemispheres [98]. Results of these experiments enabled researchers to elaborate several groups of models which may, in principle, explain the phenomena observed. Some of these models will be considered below.

5.3 Visual perception and neuron coupling

What kind of couplings between the cortex neurons provides synchronisation? One of the simplest presumptions is that the synchronisation of the activity of individual portions of the cortex is attained due to global coupling of neurons. It is clear, however, that a neural network consisting of globally coupled oscillators ('all-to-all') combines the features (synchronises the oscillators) responsible for different objects simultaneously stimulating the retina. Therefore such a neural network cannot solve even an elementary problem of geometrical recognition of several identical but spatially separated objects. At the same time, the system of locally coupled oscillators must provide a good separation of the objects because the neurons excited by one object are weakly coupled to the neurons excited by another object. Evidently, it should be supposed that two types of coupling: local (only with neighbours) and global (all-to-all) couplings inside groups of neurons are realised in the cortex simultaneously. The results of the experiment described in Ref. [98], for instance, indicate the existence of global coupling.

A rather natural model of a visual cortex which agrees rather well with the experiments on cats described above [87, 89] was constructed in Ref. [99]. In the frames of this model, there exist neurons with strong reciprocal 'all-to-all' coupling (inside the group) which are anatomically identified with columns, but each group (column) is coupled only with the neighbours:

$$\dot{\Phi}_i^{nm}(t) = a_0 - \Phi_i^{nm}(t) + \delta a^{nm} + \xi_i^{nm}(t) + K_0 I^{nm}(t) + K_\Theta \sum_{m'=m\pm1} I^{nm'}(t) + K_r \sum_{n'=n\pm1} I^{n'm}(t), \quad i = 1,\ldots,N;$$

$$I^{nm}(t) \equiv \frac{1}{N}\sum_j \sum_k \delta(t - t_j^{(k)}). \tag{5.1}$$

The model (5.1) is an example of an integrate-and-fire model [100, 101] in the frames of which each neuron is regarded as an integrator of pulses coming to the input from the other neurons. In (5.1) we used the following notation: Φ_i^{nm} stands for the variable that describes the phase of the i-th neuron in the column with number nm (Φ_i^{nm} is taken to be equal to zero if it amounts to 2π); δa^{nm} is external forcing on the column with number nm; ξ_i^{nm} designates random noise: $\langle \xi_i^{nm}(t)\rangle = 0$, $\langle \xi_i^{nm}(t)\xi_j^{n'm'}(t')\rangle = 2D\delta_{nn'}\delta_{mm'}\delta_{ij}\delta(t-t')$. The constants K_0, K_Θ and K_r have the sense of the values of coupling in one column and between neighbouring columns in two directions, respectively; and $t_j^{(k)}$ is the instant of the generation of the k-th pulse by the j-th neuron.

A scheme of a lattice that consists of 8 hypercolumns (index n) each containing 8 columns (index m) is given in Fig. 17a. It is supposed that, in each hypercolumn (n = const), different columns model the neural populations responsible for different directions of motion, i.e. having different orientation preferences but corresponding to the same portion of the retina. Different hypercolumns, in turn, model the populations bounded with different portions of the retina. Such a system allows one, to a certain extent, to model the conditions of the experiments described above.

Computer analysis of (5.1), that includes computation of the cross-correlation functions between the oscillations in different columns, gave (see Fig. 17b) the following results: (i) stimulation produces oscillatory activity in the corresponding columns; (ii) all the oscillators in one column oscillate synchronously; (iii) the groups of columns (m = const, $n \in [n_1, n_2]$) stimulated simultaneously, which corresponds to perception of an extended object, oscillate synchronously; (iv) when two space-separated groups of columns ($m^{(1)}$ = const, $n^{(1)} \in [n_1^{(1)}, n_2^{(2)}]$, $m^{(2)}$ = const, $n^{(2)} \in [n_1^{(1)}, n_2^{(2)}]$, $m^{(1)} \neq m^{(2)}$) are stimulated simultaneously, which corresponds to perception of two short objects, the oscillations are synchronous inside each group but there is no synchronism between the groups.

Similar results were obtained in investigations of another model [102] — a two-dimensional lattice of Wilson–Cowan neuron-oscillators with excitatory delayed coupling between close neighbours (Fig. 18a). Each element of this lattice is described by equations of the form

$$\tau_0 \dot{v}^e(t) = -\alpha^e v^e(t) - w^{ie} F\left[v^i(t-\tau^{ie})\right] + i^e(t) + \eta^e(t),$$
$$\tau_0 \dot{v}^i(t) = -\alpha^i v^i(t) + w^{ei} F\left[v^e(t-\tau^{ei})\right] + \eta^i(t). \tag{5.2}$$

Here $v^e(t)$ and $v^i(t)$ characterise the activity of the excitatory and inhibitory neurons, α describes the relaxation time; τ is the synaptic delay; w is the value of synaptic coupling ($w > 0$); $i^e(t)$ is the external stimulus related to the presence of the object in the field of vision, and $\eta(t)$ is weak white noise with dispersion $V[\eta(t)] = \beta^2\tau_0/12$, where β is the noise level. The condition ($\tau_0 \approx 0.5$ ms) $\ll$ ($T \approx 20$ ms), where T is the period of typical oscillations, is fulfilled. The function of synaptic coupling has the form of the Fermi function

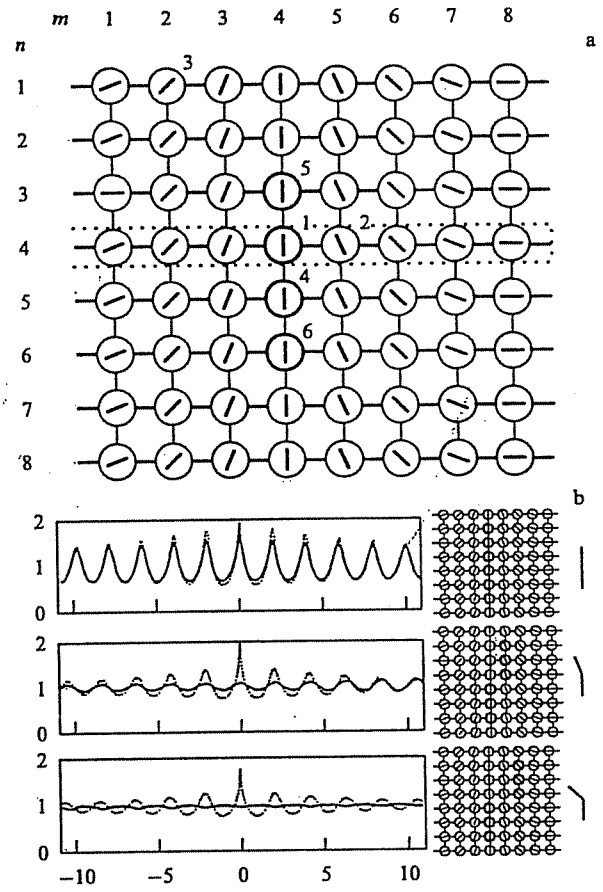

Figure 17. (a) Two-dimensional lattice which consists of 64 columns described by equation (5.1). Each circle with an oriented segment inside belongs to column m. The changes in the index n corresponds to changes in the hypercolumns which correspond to different parts of the retina. The black circles indicate the columns forced by the stimulus ($\delta a \neq 0$). (b) The response of the system (5.1) on the stimulus by two different objects of different orientations [99].

$$F[v(t)] = \frac{1}{\exp\{\sigma[\Theta - v(t)]\} + 1}, \tag{5.3}$$

where σ characterises its slope, and Θ its threshold. Note that the system (5.2), actually, describes not an individual neuron but a population of neurons possessing strong inner reciprocal couplings (see, e.g., Ref. [103]).

In the two-dimensional lattice of interest, each excitatory element v_{jl}^e is coupled synaptically to the eight neighbouring inhibitory elements $v_{j\pm1,l\pm1}^i$. Then, the complete model is written as

$$\tau_0 \frac{dv_{jl}^e}{dt} = -\alpha^e v_{jl}^e(t) - w^{ie} F\left[v_{jl}^i(t-\tau^{ie})\right] + i_{jl}^e(t) + \eta^e(t) + \sum_{\substack{j'=j\pm1\\ l'=l\pm1}} w_1^{ie} F\left[v_{j'l'}^i(t-\tau_1^{ie})\right],$$

$$\tau_0 \frac{dv_{jl}^i}{dt} = -\alpha^i v_{jl}^i(t) + w^{ei} F\left[v_{jl}^e(t-\tau^{ei})\right] + \eta^i(t) + \sum_{\substack{j'=j\pm1\\ l'=l\pm1}} w_1^{ei} F\left[v_{j'l'}^e(t-\tau_1^{ei})\right]. \tag{5.4}$$

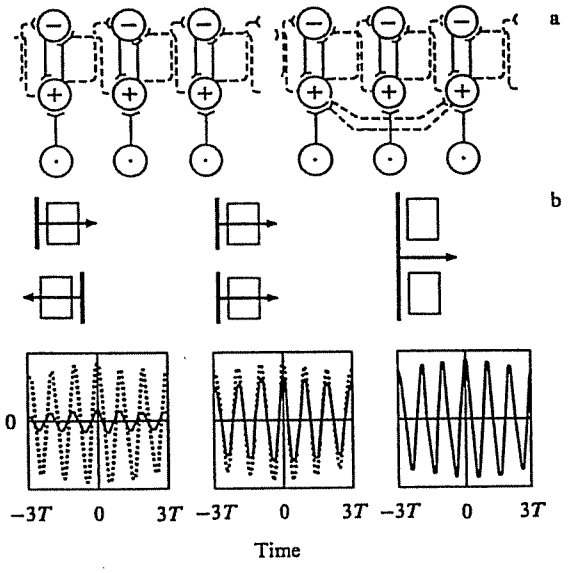

Figure 18. Three coupled two-dimensional lattices of the Wilson–Cowan oscillators. (a) The scheme on the left depicts three neighbour elements from the same two-dimensional lattice. ⊕ is excitatory coupling, ⊖ is inhibitory coupling, and ⊙ is external stimulus. The complete synchronisation is provided by delayed synaptic coupling of an excitatory neuron with neighbour inhibitory neurons (dashed line). On the right, the neighbour elements from three different lattices are shown that are described by (5.4). The delayed coupling provides synchronisation with a constant phase lag. (b) The response of three coupled lattices to two segments moving in different directions, two segments moving in the same direction and one single bar moving over two receptive fields. In lower plots, auto-correlation functions within segments (dotted lines) and cross-correlation functions between segments (solid lines) of the lattices subjected to strong external stimuli are shown [102].

Here the synaptic coupling w_1 is supposed to be isotropic. Computer experiments on such a lattice as well as on the lattice in which the elements were coupled not only with the eight nearest neighbours but also with the neighbours of their neighbours were carried out in Ref. [102]. When one group of neurons was stimulated ($i^e_{jl} \neq 0$, $j_1 \leqslant j \leqslant j_2$, $l_1 \leqslant l \leqslant l_2$), the neurons were excited and oscillated synchronously. Stimulation of two space-separated groups resulted in synchronous oscillations of neurons inside each group. However, the oscillations in the groups were phase shifted, with the phase difference decreasing as the distance between the groups in the lattice was decreased.

The model (5.4) may serve as a structural unit for more complicated models. For instance, a system of three coupled lattices each of the form (5.4) was considered in Ref. [104] (Fig. 18a). These lattices were supposed to have different orientation preferences relative to the direction of motion of the stimulating object. Two lattices corresponded to forward and backward motions, and the third one had no orientation preference (neutral lattice). The couplings between the neighbouring elements in one lattice (left) and between the elements of three different lattices (right) are shown in Fig. 18a. Note that, if the delayed coupling from the excitatory neuron to the neighbouring inhibitory one is synchronising, then the same coupling between the neighbouring excitatory neurons may give rise to desynchronisation of oscillations in nerve cells [104].

The main result of investigations of this three-layer model (Fig. 18b) is that when stimulated by two objects moving in one direction (the more so by one extended object), the oscillations excited in different lattices are synchronous. When a system is stimulated by two objects moving in opposite directions, the oscillators in different layers perform reciprocally non-synchronised oscillations. These results model correctly the observations in a cat cortex [89].

The analysis of the models (5.1)–(5.4) (as well as close results obtained in Refs [105, 106]) shows one possible way for the solution of two problems of vision: separation of the objects of one visual scene by their location in space and separation of the objects having different directions of motion. The first problem is solved successfully in a single lattice of locally coupled oscillators. Each element of this lattice corresponds to a definite portion of retina on stimulation of which a neuron or a group on neurons demonstrate oscillatory activity. Synchronous oscillations (with a zero phase shift) between spatially separated elements mean that these elements are stimulated by the same object. The larger the phase difference of oscillations between the elements of the lattice, the greater the distance between the stimulating objects is.

Note that different objects of the same retina may be separated by analyzing only spatial position of active (oscillating) and passive neurons, independent of the phase differences of their oscillations. It is significant, however, that synchronous activity of two spatially separated neurons allows one to identify their coupling with one object directly, i.e., without analysis of the state of the neurons between them.

The solution of the two problems of visual perception of objects specified above involves analysis of a series of lattices (or a chain) of oscillators coupled vertically. Each lattice must have its orientation preference, with the neighbouring elements of two lattices being associated with the same retina element. For example, a system of eight elements having different orientation preferences was considered in Ref. [99]. Each element was a one-dimensional lattice, i.e., one-dimensional visual scenes were investigated. As noted above, two-dimensional fields were considered in Ref. [104], but the authors of that work took into account only two types of orientation preferences (forwards or backwards).

Synchronous oscillatory activity of groups of neurons of several neighbouring layers means that they are stimulated only by one object moving in a definite direction that is close to the orientation preferences of these layers. A constant phase shift of oscillations in different layers indicates that the visual scene contains several objects moving in different directions. Such objects may be separated even if their positions in space are close or coincide.

In conclusion it should be noted that a complete three-dimensional model that considers both a two-dimensional visual scene (oscillator lattice) and different directions of motion of external objects (variation of orientation preference in the transition from one layer of the lattice to another) solves several problems of visual perception simultaneously and is, obviously, very interesting. Evidently, of greatest significance in such models is the structure of couplings between the neurons rather than the features of their individual dynamics.

5.4 Global competition and local synchronisation

Thus, synchronisation in the cortex stimulated externally includes two essential processes: synchronisation (with zero phase shift) of the neurons corresponding to one object and desynchronisation of the groups of neurons storing and processing the information about different objects. If several

objects are in the field of vision, then each of them in the cortex corresponds to their own groups of synchronised neurons, while the groups corresponding to different objects oscillate independently. The independence, however, does not mean non-synchronisation: the phases of oscillations in different groups may occasionally be close. The probability of such a coincidence is rather high because very many objects may stimulate the retina simultaneously. Besides, noises and the finiteness of the time spent on recognition of the objects demand to allow for the spread of parameters of the oscillations inside the group corresponding to one object. It is clear that the features corresponding to one object must correlate even if the oscillations of the corresponding neurons are not quite synchronous. This too increases the probability of coincidence of oscillations in different groups. Thus, the process of recognition of images may be prone to errors. In real life, however, this occurs rather seldom (illusions). Consequently, there must exist a mechanism responsible for stable desynchronisation of oscillations of the groups of neurons corresponding to different objects. Global competition of the oscillations between groups of locally synchronised neurons may follow such a mechanism [107, 108].

A model for a neural network in the frames of which this mechanism is carried on was proposed in Ref. [107]:

$$\dot{x}_i = 3x_i - x_i^3 + 2 - y_i + \eta + I_i + S_i\,, \tag{5.5a}$$

$$\dot{y}_i = \epsilon\left[\gamma\left(1 + \tanh\frac{x_i}{\beta}\right) - y_i\right], \tag{5.5b}$$

$$\dot{Z} = \Phi(\sigma_\infty - Z)\,, \tag{5.5c}$$

$$S_i = \sum_{k\in N(i)} w_{ik} S_\infty(x_k, \Theta_x) - w_z S_\infty(Z, \Theta_{xz})\,, \tag{5.5d}$$

$$S_\infty(x, \Theta) \equiv \frac{1}{1 + \exp[-K(x - \Theta)]}\,. \tag{5.5e}$$

Equations (5.5a,b) describe the dynamics of excitatory (x_i) and inhibitory (y_i) cells. Equation (5.5c) characterises the activity of the global inhibitor (Z) (see Fig. 19a). Finally, (5.5d,e) describe the coupling between the cells forming the lattice. The notation adopted in (5.5) are as follows: η is Gaussian noise; I_i is the external simulation; w_{ik} is the synaptic weight between the i-th and k-th oscillators; w_z is the synaptic weight between the global inhibitor and the rest of the lattice; and the set $N(i)$ describes the four nearest neighbours of the i-th neuron. In Eqn (5.5c), $\sigma_\infty \equiv 0$, if $x_i < \Theta_{zx}$ for all i, and $\sigma \equiv 1$, if $x_i > \Theta_{zx}$ at least for one oscillator; Θ_{zx} is the threshold. If the activity of all the oscillators is below the threshold, then the global inhibitor is not excited. Consequently, $Z \to 0$ and the oscillators in the lattice are not inhibited. Otherwise, if the activity of at least one oscillator is above threshold Θ_{zx}, then $Z \to 1$ and all the oscillators in the lattice are inhibited.

The characteristic features of the model (5.5) are local excitatory coupling and global inhibitory feedback, which is responsible for desynchronisation of groups of oscillators carrying information about different objects.

Numerical simulation of the system (5.5) shows that each space-separated object (the sun, tree and mountain in Fig. 19b [107]) at the input (variable I_i) of the system (5.5) corresponds to its own group of synchronised oscillators. It is significant that the oscillations in different groups are desynchronise and have a stable reciprocal phase shift (Fig. 19c). The described features of the model (5.5) agree rather well with the data

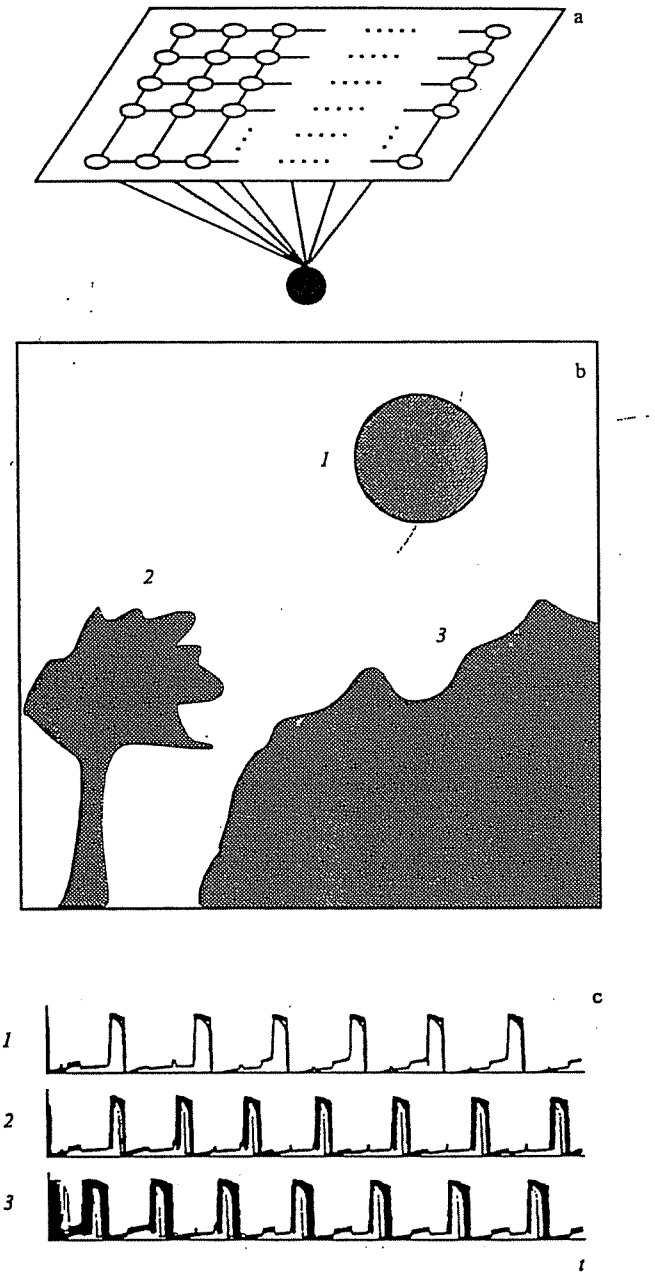

Figure 19. (a) Architecture of two-dimensional neural network with local coupling between its elements (o) and a global coupling from one inhibitor unit (•). (b) The visual image, which consists of three objects (sun (*1*), tree (*2*) and mountain (*3*)), was used as a stimulus of the system (5.5). (c) Time dependence of the oscillations in each segment of the lattice corresponding to different stimulus objects. Oscillations of all neurons belonging to the same segment is almost synchronous. However, there exists constant phase shift between different segments [107].

obtained by neurophysiologists. As was mentioned above, the lateral (or 'neighbour-to-neighbour') coupling between groups of neurons is typical of the structure of the cortex. Being the prototype of global inhibitor, the thalamus (the subcortical portion of the brain responsible for primary processing of visual information) acts on the greatest portion of the cortex at once.

The model (5.5) solves only one problem, namely, the problem of segmentation, but does not clarify the problem of binding the features into an integral image.

A step in this direction is the model proposed in Ref. [109]. Its structural unit is a lattice of Wilson–Cowan oscillators. A complete system consists of two lattices of the form

$$\frac{dm^k_{1,2}}{dt} = -m^k_{1,2} + F(Am^k_{1,2} - Bm^I_{1,2} - \Theta^E - br^k_{1,2} + i^k_{1,2}),$$
$$\frac{dr^k_{1,2}}{dt} = \left(\frac{1}{c} - 1\right) r^k_{1,2} + m^k_{1,2},$$
$$\frac{dm^I_{1,2}}{dt} = -m^I_{1,2} + F(CM_{1,2} - Dm^I_{1,2} - \Theta^I - \lambda m^I_{2,1}). \quad (5.6)$$

Here subscripts 1 and 2 refer to the 1-st and 2-nd lattice, respectively; k is the number of the oscillator in the lattice; $M_{1,2} = \sum_k m^k_{1,2}$; F is the Fermi function (5.3); $m^I_{1,2}$ and $m^k_{1,2}$ are the variables describing activity of the inhibitory and of the k-th excitatory cells (group of cells), respectively; and Θ^I and Θ^E are the threshold constants for excitatory and inhibitory neurons. This model has the following typical features: (i) threshold values for excitatory neurons contain both constant (Θ^E) and variable ($-br^k_{1,2}$) components; (ii) each of the two lattices contains N excitatory neurons and only one inhibitory neuron. Thus, each lattice contains a global inhibitor whose role is to provide competition of the ensembles of neurons excited by different objects.

In the absence of couplings between the lattices ($\lambda = 0$), the system (5.6) behaves like the model (5.5). The objects that are sent to the input simultaneously (the variable $i^k_{1,2}$) are separated in time series, i.e., the ensembles of synchronised oscillators corresponding to them are phase shifted with respect to each other.

It is supposed that in the presence of coupling ($\lambda \neq 0$) two lattices describe different features (e.g., shape and colour) of the objects which are sent to the input simultaneously. There exists an interesting idea of correct binding of the features of one object. Suppose that all the signals at the input of the system (5.6) contain noise components which are correlated for the signals containing different features of the same object and uncorrelated for different objects. Then we have

$$i^k(t) = 0.1 + 0.1[\rho^k(t) - 0.5], \quad (5.7)$$

where ρ^k is a random value in the interval (0,1) and $i^k_{1,2} = i^k$, i.e. the same signal is used for different attributes of one object.

Numerical simulation of the system (5.6), (5.7) shows that, after a short transient process, groups of oscillators belonging to different lattices and describing different features of one object are reciprocally synchronised (Fig. 20). At the same time, a constant phase difference is established between the groups of oscillators corresponding to different objects. The described model solves, in the simplest form, two problems: segmentation and binding of images. Note that the role of noise is not restricted to binding in such models. The noise, additionally, increases the number of the objects that may be segmented simultaneously. The latter was confirmed in Refs [109, 116]. We would also like to add that analysis indicates that the probability of errors grows with an increase in the number of objects sent to the input simultaneously: the groups of oscillators responsible for different objects become synchronised, which gives rise to illusions.

A rather general three-dimensional model (5.4) of visual cortex that was analyzed in Section 5.3 considers an object features such as its geometrical position and the direction of motion. This model takes into account local couplings between the elements and assures synchronous oscillatory

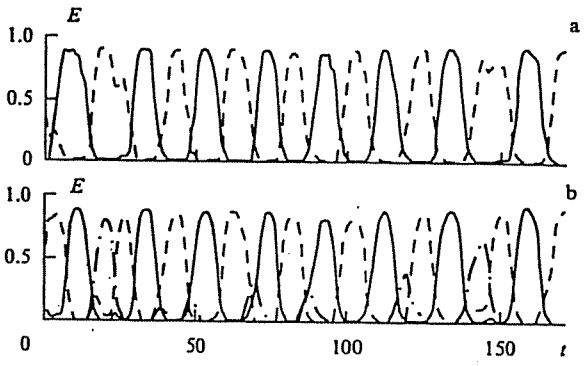

Figure 20. Time dependence of oscillatory activity in two groups (solid and dashed lines) of excitatory neurons when the system (5.6), (5.7) is stimulated by two different objects. The dashed line represents activity of neurons that have not been stimulated. Pictures (a) and (b) show oscillations in different lattices for different features of the input object (for example, shape and colour). There is a constant phase shift between oscillations of neurons in the same lattice stimulated by different objects. However, the phase shift between oscillations of the neurons corresponding to different features (different lattices) of the same object is equal to 0 [109].

activity of all the neurons bounded with each object of the visual scene. Bearing in mind the role of global inhibitor in providing constant phase shift of oscillations between different groups of excited neurons, the model (5.4) must be supplemented with global feedback. The latter will provide reliable separation of the objects having different spatial coordinates and directions of motion.

Systems with local excitatory and global inhibitory couplings of elements are encountered not only in modelling visual cortex. This situation is also typical of many processes of pattern formation. The principle of local excitation and global inhibition is employed in the nature for the formation of stable spatial structures in different variants and at different levels. It is one of the basic principles of the initial stage of morphogenesis, in which local catalysis plays the role of local excitation, and long-term inhibition may be associated, for instance, with fast inhibitor diffusion [110]. An analogous principle is realised in multicomponent chemical Belousov–Zhabotinsky reactors and in segregation in colonies of bacterias and amoebas [111, 112]. Local excitation (or local synchronisation) supported by global competition lead to formation of stable localised structures both in Rayleigh–Benard convection [113] and in nonequilibrium optical media [114].

5.5 Synchronisation and associative memory

The problem of perception (visual, auditory, etc.) is, evidently, related to memory. Memory is usually classified as short- and long-term one. Short-term memory lasts for about 10 to 20 minutes, after which the information stored in it is lost, unless transformed to long-term memory as a result of some stimulation (e.g., purposeful concentration of attention). We have already mentioned that, according to one of the popular hypotheses (see, e.g., Ref. [115]), the mechanism of long-term memory consists of structural changes of synaptic couplings between neurons, whereas short-term memory is related to formation of metastable structures of neural activity. These may be, for instance, groups of synchronised neurons. In the context of such models, different synchronisation patterns in the neural network correspond to different

images stored in short-term memory. The state of the network is supposed to depend on the parameters that change with the characteristic time of the order of the time of short-term memory. When this time has elapsed, the neural network acquires an unexcited state, and the information stored in it is lost, unless an additional stimulus transforms the temporal synchronisation of the group of neurons to a constantly acting one by forming new synaptic couplings. The network passes from the metastable to the stable state: still another attractor appears in the phase space of the dynamical system describing long-term memory. The existence of a finite attraction basin of such attractors enables the system to recognise not only the image identical to the one memorised before but also a slightly distorted or incomplete image. This is the associative feature of long-term memory.

Judging from the available experimental data, associative memory is not capable of using different functional components of the memorised object in new combinations. Any complex object is memorised as a whole and the memory reconstructs either the object as a whole or nothing. Therefore even the visual scenes consisting of identical elements with different locations are memorised independently.

In perception of any complex object the response occurs simultaneously in many portions of the cortex responsible for processing the various characteristics of the object. This means that the object is memorised as a whole (the character of synaptic couplings is changed) and in many portions of the cortex simultaneously. Thus, there again arises the problem considered above: stimulation must provide simultaneous synchronous oscillations of several groups of neurons responsible for different features of the object memorised before. These groups of neurons must be excited simultaneously on repeated perception of the object that is identical or close (associations) to the remembered one. The models proposed for solution of this problem are similar to those considered in Sections 5.3 and 5.4. However, they have a number of distinguishing features one of which will be analyzed in more detail.

Consider a neural network [116] the elements of which are Wilson–Cowan oscillators of the form

$$\frac{dx_i}{dt} = -\frac{x_i}{\tau_x} + F_x\left[T_{xx}\frac{x_i}{\bar{x}} - T_{xy}G\left(\frac{y_i}{\bar{y}}\right) + S_i + I_i - H_i\right],$$

$$\frac{dy_i}{dt} = -\frac{y_i}{\tau_y} + F_y\left[-T_{yy}\frac{y_i}{\bar{y}} + T_{yx}\frac{x_i}{\bar{x}}\right],$$

$$H_i = \alpha\int_0^t x_i(\tau)\exp\left[-\beta(t-\tau)\right]d\tau, \qquad i = 1,\ldots,N. \quad (5.8)$$

Here x_i and y_i are average activities of the i-th excitatory and inhibitory cells, respectively; F_x and F_y are the Fermi functions (see (5.3)) with constant Θ_x, τ_x, and Θ_y, τ_y, respectively; H_i describes the delayed self-inhibition; and the function $G(x) = (1-\eta)x + \eta x^2$ $(0 \leqslant \eta \leqslant 1)$ is chosen for increasing the structural stability of the system (5.8) as the parameters are changed. The parameters $\bar{x}$ and $\bar{y}$ are used to control the average values of x_i and y_i. The variable $I_i(t)$ describes external action, and $S_i(t)$ the action of other neurons of the network:

$$S_i(t) = \sum_{k\neq i} w_{ik}x_k(t), \quad (5.9)$$

where w_{ik} are synaptic weights.

Suppose that we have p different patterns: $\xi^\nu = [\xi_i^\nu]_{i=1}^N$, $\nu = 1,\ldots,p$. Each pattern may be regarded as a one-dimensional visual scene consisting of contrast objects (points $\xi_i^\nu = 1$) and background ($\xi_i^\nu = 0$), i.e.,

$$\xi^1 = (1,1,1,1,1,1,1,1,0,0,0,0,0,0,0,0,0,0,0,1,0,\ldots,0),$$
$$\xi^2 = (0,0,0,0,0,0,1,1,1,1,1,1,1,1,0,0,0,0,0,0,1,0,\ldots,0),$$
$$\xi^3 = (1,0,0,0,0,0,0,0,0,0,0,0,1,1,1,1,1,1,1,1,0,\ldots,0). \quad (5.10)$$

For memorising such visual scenes by a neural network consisting of N oscillators we choose the strength of synaptic coupling following the Hebbian rule that determines w_{ik} as a function of multiplication of stimuli [30, 117]:

$$w_{ik} = \frac{1}{aN}\sum_\nu(\xi_i^\nu - a)(\xi_k^\nu - a), \quad (5.11)$$

where a is the probability that $\xi_i^\nu = 1$ (a is usually taken to be smaller than 0.2).

Principal results of modelling the system (5.8)–(5.11) are the following [116]. If the pattern $\bar{\xi}^\nu$ that is similar to one of the patterns stored in the system ξ^ν, i.e. $I_i = c\bar{\xi}_i^\nu$, $0 < c < 1$, is sent to the input of the system, then all the neurons, for which $\xi_i^\nu = 1$, are excited and oscillate synchronously. All the other neurons remain unexcited. In this fashion the system has at its output the stored visual scene ξ^ν. Let us now send to the input a superposition of three patterns $\bar{\xi}^1$, $\bar{\xi}^2$, $\bar{\xi}^3$ that are close to the previously remembered structures (5.10):

$$I = c(1,0,1,1,1,1,1,1,0,1,1,1,1,1,1,0,1,1,1,1,1,1,0,\ldots,0).$$

Note that the input signal will correspond exactly to the superposition (5.10) if we set $I_2 = I_8 = I_{14} = 1$. Such a stimulation excites three groups of synchronously oscillating neurons that correspond to three patterns at the input. Each pattern coincides exactly with the ones memorised before, i.e., the error of the input signal is corrected. It is significant that the groups of neurons corresponding to different patterns (visual scenes) have a constant phase shift. Thus, only one group of neurons has maximal activity at each time instant. Consequently, the system (5.8)–(5.11) separates the patterns at the input and demonstrates them one after the other if these patterns coincide or are close to the structures stored in the synaptic couplings between the neurons, i.e., remembered by the neural network. Note that the proposed model also works for the case of partial overlapping of the patterns at its input when $\xi_i^\nu = \xi_i^\mu = 1$, $\nu \neq \mu$. However, if the number of the patterns at the input is large ($p \geqslant 10$ in this case), then they are no longer separated and irregular oscillations are observed at the output.

It is interesting to compare the above model of associative memory on oscillating elements with the gradient model proposed in Ref. [118]. Such a model may be represented in a simplified form as

$$\frac{dx(\mathbf{r},t)}{dt} = -\frac{\delta V(x)}{\delta x}, \quad (5.12)$$

where $V(x)$ is the free energy functional decreasing along the trajectory of the system and $\mathbf{r}$ is the spatial coordinate of the lattice element. For arbitrary initial conditions, the system (5.12) evolves to one of the nearest local minima in the coordinates 'free energy functional — stationary state of the

lattice' and stays there for an infinitely long time, provided there are no perturbations. These minima may be formed as a result of the changes of synaptic coupling between the elements in the lattice in the course of learning. Thus, each minimum may be regarded as an image stored by associative memory. The transition of the system (5.12) to a stable state associated with this minimum is actually a process of recognition. The basic difference between the Hopfield model (5.12) and the model (5.8)–(5.11) is that the latter is constructed from oscillating elements.

Of course, the model (5.8)–(5.11) does not pretend to be exhaustive and universal. However, in the framework of this model one can successfully solve the problem of long-term storage of images and their classification according to the memorised information that is very significant for associative memory (see also Refs [119, 120]).

5.6 Spatio-temporal synchronisation structures

When discussing the dynamics of a homogeneous neural network, we considered the case when the neurons activated by external stimulus are excited and oscillate synchronously with a zero phase difference in one or several groups corresponding to the same stimulus, while the other (disactivated) neurons are in an unexcited state. It is quite possible, however, and in many cases even inevitable, that the cells which are not stimulated directly may be excited when a group of neurons or even a single neuron are stimulated. It is known, for example, that periodic stimulation of a single point on the surface of the cortex produces an epileptic fit, i.e. generates complex spatio-temporal patterns of electric activity in a very large volume of the cortex, and these patterns are retained after the stimulation has ceased [121, 122].

Excitation of the cells which do not experience direct external forcing occurs due to the couplings between them and, in the case of nonglobal coupling, resembles a wave propagating in space. It is important that the type of activity of the excited neurons (the phase shift between the neighbouring cells, and so on) is determined in this case not by the external stimulus but by the features intrinsic in the network and, primarily, by the type of the coupling of its elements. It is natural to suppose that there may appear the states when the excited neurons oscillate synchronously but the phase differences between the neighbouring cells are non-zero and depend on their spatial location in the lattice, i.e, complex spatially inhomogeneous structures may be formed. Such structures (spiral or plane waves, envelope solitons, etc.) have been observed in many models of active nonequilibrium media of different origins: physical, chemical, biological, and so on. Below we will consider in the frames of models of neural networks stable existence of one of the most nontrivial structures of this type, namely, a spiral wave.

Spiral waves were investigated theoretically in ample detail in the framework of the Ginzburg–Landau model (see, e.g., Ref. [72]):

$$\dot{a} = a + (1 + \mathrm{i}\alpha)\nabla^2 a - (1 + \mathrm{i}\beta)|a|^2 a, \tag{5.13}$$

that has the exact solution [115]

$$a(r, t) = F(r)\exp\{\mathrm{i}[-\omega t + m\phi + Q(r)]\}, \tag{5.14}$$

corresponding to a spiral wave with topological charge m. Here r and ϕ are polar coordinates; $F(r)$ and $Q(r)$ are known functions. The model (5.14) is especially attractive because it describes spatio-temporal dynamics of an arbitrary space-extended system near the critical value of the parameters corresponding to the birth of large-scale single frequency oscillations (The Hopf bifurcation) [72].

The self-sustained spiral waves may arise, in particular, in excitable biological tissues [123, 124]. For example, travelling spiral waves were observed in cardiac [125, 126] and nerve [127, 128] tissues. The authors of Ref. [129] observed and investigated the spiral waves in a lattice of diffusively coupled neuron oscillators of the Morris–Lecar type (see Section 1.2). In all these works homogeneous media in which the spirals were generated by means of special initial conditions were considered. The propagating spiral waves may also be produced by point stimulation of an inhomogeneous medium with homogeneous initial conditions when there are no atomic barriers [20, 130]. The latter possibility was analyzed in Ref. [131] based on a model for a neural network consisting of integrate-and-fire neurons. We will consider these results in more detail.

The dynamics of such a neuron model is described as follows. Each neuron has a threshold $\Theta(t)$ and is excited if the membrane potential exceeds this threshold, otherwise the neuron is not activated. On being excited the neuron generates a spike, after which its membrane potential $M(t)$ drops to some constant value M_0. The variations of the membrane potential between two spikes meet the equation

$$\tau\frac{\mathrm{d}M}{\mathrm{d}t} = -M + R(I^{\mathrm{syn}} + I^{\mathrm{ext}}), \quad \text{if} \quad 0 < M < \Theta,$$
$$M(t_0 + 0) = 0, \quad \text{if} \quad M(t_0 - 0) = \Theta, \tag{5.15}$$

where τ is the time constant; I^{syn} and I^{ext} are the variables which describe, respectively, the synaptic coupling with the other cells and external excitation. The variation of the threshold $\Theta(t)$ in time is given by the expression [132]

$$\Theta(t) = \Theta_0 + \frac{\exp[-K_\Theta(t - t_f)]}{1 - \exp[-K_\Theta(t - t_f)]}, \tag{5.16}$$

where t_f is the time instant corresponding to the last burst of the neuron activity.

It was supposed that the average number of couplings between two neurons, $\lambda(r)$, is an exponentially decaying function of the interneuron distance r in the lattice [133]

$$\lambda(r) = \beta\exp(-\alpha r), \tag{5.17}$$

where α and β are some constant values. The probability that there exist q couplings between two neurons obeys the Poisson law

$$P_q(r) = \frac{\lambda(r)^q \exp[-\lambda(r)]}{q!}. \tag{5.18}$$

The authors of Ref. [131] took as the initial conditions unexcited states of all the neurons, one of which was stimulated externally. Under these conditions, first, a cylindrical structure is formed in the system, then it breaks and a spiral wave arises. The neurons with synchronous oscillatory phases correspond to the fronts of this spiral wave. The formed spiral waves are retained even after external stimulus has ceased, i.e., we can say that they are stable eigenmodes of a neural lattice.

Spiral waves were also revealed in the framework of another model of neural network consisting of N excitatory and M inhibitory cells [134]. For description of the dynamics of the membrane potential of the i-th excitatory (x_i) and of the j-th inhibitory (y_j) neurons the following equations were chosen

$$\frac{dx_i}{dt} = -\gamma(x_i - V_L) - (x_i - V_E)\omega_1 \sum_k F\big(x_k(t-\tau_{ki})\big) - (x_i - V_I)\omega_2 \sum_l F\big(y_l(t-\tau_{li})\big),$$

$$\frac{dy_j}{dt} = -\gamma(y_j - V_L) - (y_j - V_E)\omega_3 \sum_k F\big(x_k(t-\tau_{kj})\big) - (y_j - V_I)\omega_4 \sum_l F\big(y_l(t-\tau_{lj})\big),$$

$$i = 1,\ldots,N; \quad j = 1,\ldots,M. \quad (5.19)$$

Here V_L is the leakage potential; V_E and V_I are the equilibrium potentials of synaptic excitation and inhibition, respectively; ω_α ($\alpha = 1,2,3,4$) are the constants of synaptic coupling between the neurons; and τ_{ij} are the delays which depend on the distance between neurons. The authors of Ref. [134] considered two types of coupling between the neurons: (1) only to the nearest neighbours and (2) to the nearest neighbours and to the neighbours of their neighbours. Lattices of two types were investigated: (i) with equal number of excitatory and inhibitory cells and (ii) with predominance of excitatory cells.

Dynamics of the system (5.19) without external stimulation was investigated. It was found that, for certain values of the parameters, a stable structure in the form of a spiral wave is formed in the lattice with a rather great amount of neurons. In terms of neurophysiology, this spiral wave is a depolarisation wave propagating in the lattice. Some cells are depolarised and the others are hyperpolarised in the neighbourhood of depolarisation front. It is interesting that, if the size of the lattice exceeds a definite critical number, then defect mediated turbulence arises in the system [135]. This process is accompanied by formation of a great number of depolarisation fronts propagating in different directions which emerge spontaneously and collapse on collisions with each other.

Analysis of the models considered above shows that, in spite of the trivial (oscillatory) dynamics of individual neurons, their collective behaviour may be quite diverse and complicated. Patterns of reciprocally synchronised neurons having a complex spatial form and nontrivial dependence of oscillatory phases of individual cells on coordinates may arise in the system. On the other hand, when external stimulation occurs (e.g., stimulation of the retina of the visual cortex), the collective dynamics of neurons becomes simpler and more ordered. According to one of the hypotheses [136], the intrinsic complex spatio-temporal dynamics of neural ensembles of the cortex is responsible for the sensations (visual, auditory, etc.) which a human being has in his (her) sleep when external stimulation is minimal. Of course, neural ensembles of the cortex are not, actually, homogeneous. Their synaptic couplings bear information about the objects stored in long-term memory. But, perhaps, that is the reason why the images arising in dreams are not absolutely irregular but, instead, include quite real (stored in memory) objects and events.

6. Conclusions

To conclude it can be stated that the mechanisms controlling rhythmic activity of living organisms are connected with synchronisation of the interacting neurons that form the corresponding CPGs. Central pattern generators should be regarded as a nonlinear dynamical system. There is noise in such a system but it performs a rather definite function, namely, inhibiting various exotic regimes of operation of CPGs whose region of stability is negligibly small. Of course, there are still many gaps in the general picture of CPG functioning. However, a general understanding of the

Table. Models of neurons

Model (year)	Basic equations	Basic variables	Remarks	References
1. Hodgkin, Huxley (1952)	$C\frac{dv}{dt} = I - g_{Na}m^3h(v-v_{Na}) - g_K n^4(v-v_K) - g_L(v-v_L)$, $\frac{dm}{dt} = \frac{m_\infty(v)-m}{\tau_m(v)}$, $\frac{dh}{dt} = \frac{h_\infty(v)-h}{\tau_h(v)}$, $\frac{dn}{dt} = \frac{n_\infty(v)-n}{\tau_n(v)}$	v — membrane potential, m and h — variables to describe openings and closings of Na^+ ionic channels, n — variable to describe openings and closings of K^+ ionic channel; g_{Na}, g_K, g_L — conductances for sodium, potassium and leaking currents, v_{Na}, v_K, v_L — reverse potentials for corresponding currents; c — membrane capacitance	These equations describe squid's giant axon. The parameter values and functions m_∞, h_∞, ... can be found in Ref. [138]	[14, 138]
2. Connor, Walter, McKown (1977)	This model has an additional current to the previous one, given by $I_A = -g_A(v-v_A)A^3B$, $\frac{dA}{dt} = \frac{A_\infty(v)-A}{\tau_A(v)}$, $\frac{dB}{dt} = \frac{B_\infty(v)-B}{\tau_B(v)}$		The frequency of spikes can vary much more than in the previous model	[138, 139]

Table (continued)

3. Morris, Lecar (1981)	$\frac{dv}{dt} = g_L[v_L - v] + \eta g_n[v_n - v] + + g_m m_\infty(v)[v_m - v] + I_{app}$, $\frac{dn}{dt} = \lambda(v)[n_\infty(v) - n]$, usually $m_\infty = \frac{1}{2}\left(1 + \tanh\frac{v - v_m}{v_m^{(0)}}\right)$, $n_\infty = \frac{1}{2}\left(1 + \tanh\frac{v - v_n}{v_n^{(0)}}\right)$, $\lambda = \lambda(v) = \varphi_n \cosh\frac{v - v_n}{2v_n^{(0)}}$	v — membrane potential, n — generalized variables that describe recovering of activity of one of the currents, c — membrane capacitance, I_{app} — external current. All variables in the right-hand side of the first equation describe ionic currents	This model was introduced in [104] to analyze interaction of two coupled neurons	[15, 140, 141]
4. Chay (1985)	$-C\frac{dv}{dt} = g_1 m_\infty^3 h_\infty(v - v_I) + g_K n^4(v - v_K) + + g_p P(v - v_K) + g_L(v - v_L)$, $\frac{dn}{dt} = \frac{n_\infty - n}{\tau_n}$, $\frac{dP}{dt} = \frac{m_\infty^3 h_\infty(v_I - v) - k_c P/(1 - P)}{\tau_P}(1 - P)^2$	The third term in the right-hand side of the equation describes the Ca^{2+}-dependent part of K^+ current	Three-dimensional model that describes dependence of K^+ current on Ca^{2+} ions concentration	[18, 142]
5. Chay (1990)	$C\frac{dv}{dt} = -g_{fast} m_\infty h(v - v_{fast}) - - g_{slow} df(v - v_{slow}) - g_K n(v - v_K) - - g_L(v - v_L)$, $\frac{df}{dt} = \lambda_f(1 - f) - \lambda_f \frac{[Ca^{2+}]}{k_{Ca}} f$, $\frac{dC}{dt} = \rho\left\{\frac{g_{slow} df(v_{slow} - v)}{\sigma} - k_{Ca} C + k_{Ca} C_r\right\}$, $C = \frac{[Ca^{2+}]}{k_{Ca}}$	6-dimensional system: n, d, h describe activation and inactivation like in the Hodgkin–Huxley model	The model is based on a particular hypothesis about inactivation of Ca^{2+}	[142, 143]
6. Golovasch (1990)	$C\frac{dv}{dt} = I_{ext} - \sum_j I_j$, $I_j = g_j a_j^p b_j^q (v - v_j)$, $\frac{da_j}{dt} = k_j(v)[a_{j\infty}(v) - a_j]$, $a_{j\infty}(v) = \left[1 + \exp\left(\frac{v - v_j}{s_j}\right)\right]^{-1}$	13-dimensional system based on a more detailed description of Ca^{2+} channels	Model of LP stomatogastric ganglion neuron of crab Cancer borealis	[13, 144, 145]
7. Golomb, Guckenheimer, Gueron (1993)		7-dimensional system that contains the same currents that the previous one, but currents with similar dynamics are described by similar equations for a_j, b_j	LP neuron model derived from the previous one that qualitatively describes the dynamics of the membrane potential	[145]
8. Wilson, Cowan (1973)	$\frac{dv_e}{dt} = F(v_e, n_e) + \omega_i g_i[v_K - v_e]$, $\frac{dn_e}{dt} = G(v_e, n_e)$, $\frac{dv_i}{dt} = F(v_i, n_i) + \omega_e g_e[v_{Na} - v_i]$, $\frac{dn_i}{dt} = G(v_i, n_i)$	v_e, v_i — membrane potentials, n_e, n_i — recovery variables that describe excitatory and inhibitory neurons	It models an oscillatory system that consists of 2 non-oscillatory populations of neurons	[20,141]
9. Stein, Leung, Mangeron, Oğuztöreli	$\frac{dx_i}{dt} = a\left[-x_i + \frac{1}{1 + \exp(-f_{ci} - by_i + bz_i)}\right]$, $\dot{y}_i = x_i - py_i$, $\dot{z}_i = x_i - qz_i$, $i = 1, [1 \div 2], [1 \div 3] \ldots$	x_i — membrane potential of i neural oscillator, a — a constant of time that indicates how the potential changes in time; f_{ci} — excitatory signal at i oscillator, b is a parameter that describes efficiency of adaptation to stimuli changes, p and q indicate the velocity of this adaptation	The type of coupling between neurons is defined by f_{ci}. For example, inhibitory coupling can be obtained by decreasing f_{ci} to a value proportional to the signal of inhibitory oscillator $f_{ci} = f(1 - \sum_j \lambda_{ji} x_j)$	[145, 146]

Table (continued)

10. Hindmarsh, Rose (1984)	$\frac{dx}{dt} = y + ax^2 - bx^3 - z + I$, $\frac{dy}{dt} = C - dx^2 - y$, $\frac{dz}{dt} = r[s(x - x_0) - z]$	x — membrane potential, y describes the dynamics of fast currents, a, z represents the slow current dynamic, I — the external current	Phenomenological models	[17, 19]
11. Fitz Hugh (1961), Nagumo, Arimoto, Yoshizawa (1962)	$\dot{x}_i = x_i - \frac{x_i^3}{3} - y_i + f_{ci}$, $\dot{y}_i = x_i + by_i - a$	x_i — membrane potential, f_{ci} — excitatory current. These variables are physiologically meaningful. a, b, c — empirical constants	The effect of couplings may be taken into account similarly to the previious case	[147, 148]
12. Integrate-and-fire models	$\frac{dv}{dt} = -\frac{v}{\tau_0} + I_{ext} + I_{syn}(t)$ for $0 < v < \Theta$, $v(t_0^+) = 0$ if $v(t_0^-) = \Theta$, usually $I_{syn}(t) = g \sum_{spikes} f(t - t_{spike})$, $f(t) = A\left[\exp\left(-\frac{t}{\tau_1}\right) - \exp\left(-\frac{t}{\tau_2}\right)\right]$	Θ — threshold value of potential, when v reaches this value the neuron is reset to 0. Time constant τ_0 and current I_{ext} determine fast neurons fire, I_{syn} — synaptic current	A very simple analog of the previous models. It is not based on physiology. Actually it describes the interspike interval not the spike itself	[138]
13. Van-der-Pol generator	$\ddot{x}_i + \mu(x_{ai}^2 - p^2)\dot{x}_i + g^2 x_{ai} = f(t)$, $x_{ai} = x_i + \sum_j \lambda_{ji} x_j$		By its origin, this model has nothing in common with physiology of neurons. It is used for investigation of collective behaviour of neural assemblies, that does not depend on the choice of a particular model. Sometimes, the change of variables $x_i \to x_{ai}$ is introduced to model synaptic coupling [149]	[3, 149]

situation and continuously appearing new delicate experiments on both invertebrates and higher vertebrates give optimistic prognosis for construction of a complete dynamical theory.

Much more complicated is to understand the general dynamical and information principles behind the operation of higher nervous system. In this review we have addressed problems of mapping visual scenes into patterns of dynamical activity of the cortex. Today there exist models, relating visual scenes to patterns of synchronous activity of neural ensembles in different portions of visual cortex, that do not contradict the results of experiments. These models show possible ways for solution of the problem of establishing a correspondence between excitations in the cortex and observed images. However, very little is known about how this processed and systematised information is used by the brain, how it is read by it. If a map of cortex excitations corresponding to a visual scene is regarded as a TV screen, then we can recall the words of Francis Crick: "who watches this screen?". Nevertheless, if we do not keep strictly to the problem of thinking, particularly consciousness, then we can find an answer to this question. Memory, that is itself distributed in the central nervous system, is the consumer (perhaps not the only one) of generated information. Suppose that we speak about visual images. If the new-formed image resembles the original one existing in the memory (in terms of nonlinear dynamics we can say that the computed image is in attraction basin of the known attractor-image), then from its previous experience the nervous system knows what to do with the information received. For example, a mouse in a cat's visual cortex or a bright rattle in a baby's brain. If the image is novel, then it is recorded in the memory together with the information about the experience of interaction with this object.

Using the concept of V Turchin [137] we can refer the described activity of nervous system to associations (or controlling reflexes), and its next hierarchic stage to controlling associations, namely, thinking. It is not clear yet whether this level of activity of nervous system may be described completely enough using the language of nonlinear dynamics. We do not know, in particular, how to pass from a specific image and functioning of the brain related to a definite goal that is associated with this image to abstract thinking. Evidently, a significant intermediate element is a game in this case [111, 137]. A game models a real image and a real aim, while the only thing missing here is a signal to real action. The brain itself closes the 'image — processing — comparison with memory — signal to formation of a new image' chain. It is already a close approach to abstract thinking.

The authors highly appreciate fruitful discussions with Yu Arshavsky, A Gaponov-Grekhov, P Rowat, N Rulkov, M Tai, D Trubetskov, L Tsimring, and V Yakhno.

This research was supported by the Russian Foundation for Basic Research (project code No. 94-02-03263), the International Soros Foundation (grants N.NOU000 and N.NOU300), and the International Center for Advanced Studies in Nizhniĭ Novgorod (grants No. 95-E-01 and No. 95-E-02).

References

1. Huygens H *Tri Memuara po Mekhanike* (Three Memoirs in Mechanics) (Ed. by K Baumgart) (Translated into Russian) (Moscow: Academy of Sciences of USSR Publishing House, 1951)
2. Rayleigh *Teoriya Zvuka* (Theory of Sound) Vol. 1, 2 (Translated into Russian) (Moscow: Gostekhizdat, 1940, 1944)
3. Van der Pol B *Nelineĭnaya Teoriya Électricheskikh Kolebaniĭ* (Nonlinear Theory of Electrical Oscillations) (Translated into Russian) (Moscow: Svyaz'izdat, 1935)
4. Andronov A A, Vitt A A, Haĭkin S É *Teoriya Kolebaniĭ* (Theory of Oscillations) (Translated into Russian) (Moscow: Fizmatgiz, 1959)
5. Hedley P, Beasley M R, Wiesenfeld K *Phys. Rev. B* **38** 8712 (1988)
6. Arnol'd V I et al., in *Sovremennye Problemy Matematiki. Fundamental'nye Napravleniya* (Contemporary Problems of Mathematics. Basic Directions) Vol. 5 (Ed. V I Arnol'd) (Moscow: VINITI, 1986)
7. Afraĭmovich V S, Verichev N N, Rabinovich M I *Izv. Vyssh. Uchebn. Zaved. Radiofiz.* **29** 1050 (1986)
8. Székely G *Acta Phys. Acad. Hyng.* **27** 285 (1965)
9. Afraĭmovich V S, Reĭman A M, in *Nelineĭnye Volny. Dinamica i Évolutsiya* (Nonlinear Waves. Dynamics and Evolution) (Ed. A V Gaponov-Grekhov, M I Rabinovich) (Moscow: Nauka, 1989) p. 238
10. Aranson I S, Reĭman A M, Shekhov B G Ibid., p. 262
11. Abarbanel H D I et al. *Rev. Mod. Phys.* **65** 1331 (1993)
12. Shepherd G M *Neurobiology* (Oxford: Oxford Univ. Press, 1994)
13. Buchholtz F et al. *J. Neurophysiol.* **67** 332 (1992)
14. Hodgkin A L, Huxley A F *J. Physiol.* (London) **117** 500 (1952)
15. Morris C, Lecar H *Biophys. J.* **35** 193 (1981)
16. Hayashi H, Ishizuka S *J. Theor. Biol.* **156** 269 (1992)
17. Abarbanel H D I et al. *Biol.Cybern.* (1996) (to be published)
18. Chay T R *Physica D* **16** 233 (1985)
19. Hindmarsh J L, Rose R M *Proc. R. Soc. London. Ser. B* **221** 87 (1984)
20. Wilson H, Cowan J *Kybernetic* **13** 55 (1973)
21. Ermentrout G B, Kopell N *SIAM J. Math. Anal.* **15** 215 (1984)
22. Borisyuk G I et al. *Matematisheskoe Modelirovanie* **4** 3 (1991)
23. Cuffler S, Nikkols J *Ot Neĭrona k Mozgu* (From Neuron to Brain) (Translated into Russian) (Moscow: Mir, 1979)
24. Shapovalov A I, Shiryaev B I *Peredacha Signalov v Mezhneĭronnykh Sinapsakh* (Transmission of Signals in Synapses) (Leningrad: Nauka, 1987)
25. Agmon-Snir H, Segev I *J. Neurophysiol.* **70** (5) 2066 (1993)
26. Kalil R E et al. *Nature* (London) **323** 156 (1986)
27. Voronin L L *Synaptic Modifications and Memory* (Berlin, 1993)
28. Byzov A L, Shura-Bura T M *Vision Res.* **26** 33 (1986)
29. Matyushkin D P *Obratnye Svyazi v Sinapse* (Feed-back in Synapse) (Moscow, 1989)
30. Hebb D O *The Organization of Behaviour* (New York: Wiley, 1949)
31. Hertz J, Krogh A, Palmer R G *Itroduction to the Theory of Neural Computation* (Redwood city: Addison Welsey, 1991)
32. Hopfield J J *Proc. Natl. Acad. Sci. USA* **79** 2554 (1982)
33. Hopfield J J *Phys. Today* 40–46 (1994)
34. Harris-Worrick R M, Marder E, Selverston A I *Dynamic Biological Networks* (Cambridge: MIT Press, 1992)
35. Arshavsky Yu I et al. *TINS* **16** 227 (1993)
36. Katz P S, Getting P A, Frost W N *Nature* (*London*) **367** 723 (1994)
37. Huerta P T, Lisman J E *Nature* (*London*) **364** 723 (1993)
38. Schuman E M, Madison D V *Science* **263** 532 (1994)
39. Mpitos G J et al. *Brain Res. Bull.* **21** 529 (1988)
40. Selverston A et al. (to be published)
41. Fujisaka H, Yamada T *Prog. Theor. Phys.* **69** 32 (1983)
42. Rulkov N F et al. *Int. J. Bif. Chaos* **2** 669 (1992)
43. Arshavsky Yu I et al. (to be published).
44. Delcomyn F *Science* **210** 492 (1980)
45. Grillner S *Science* **228** 143 (1985)
46. Rowell C H F *Semin. Neurosci.* **5** 59 (1993)
47. Collins J J, Stewart I N *J. Nonlinear Sci.* **3** 349 (1993)
48. Grillner S, Kashin S, in *Neural Control of Locomotion* (Eds R Herman, S Grillner, P Stein, L Stuart) (New York: Plenum Press, 1976) p. 181
49. Grillner S et al. *Semin. Neurosci.* **5** 17 (1993)
50. Grillner S *Exp. Brain. Res.* **20** 459 (1974)
51. Wallen P, Williams T L *J. Physiol.* (London) **347** 225 (1984)
52. Williams T L et al. *J. Exp. Biol.* **143** 559 (1989)
53. Timstall M J, Roberts A *Pros. R. Soc. London. Ser. B* **244** 27 (1991)
54. Paul D H, Mulloney D *J. Neurophysiol.* **54** 28 (1985)
55. Sigvardt K A *Semin. Neurosci.* **5** 3 (1993)
56. McClellan A D, Sigvardt K A *J. Neurosci.* **8** 133 (1988)
57. Rovainen C *J. Neurophysiol.* **54** 959 (1985)
58. Rabinovich M I, Trubetskov D I *Oscillations and Waves in Linear and Nonlinear Systems* (Dorderecht, Boston, London: Kluwer Academic Publ., 1989)
59. Cohen A H, Holmes P J, Rand R H *J. Math. Biol.* **13** 345 (1982)
60. Williams T L *Neural Computation* **4** 546 (1992)
61. Grillner S et al. *Annu. Rev. Neurosci.* **14** 169 (1981)
62. Weeks J C *J. Neurophysiol.* **45** 698 (1981)
63. Hashemzadeh-Gargari H, Friesen W O *Comp. Biochem. Physiol.* **94C** 295 (1989)
64. Friesen W O, Pearce R A *Semin. Neurosci.* **5** 41 (1993)
65. Grillner S, Perret C, Zangger P *Brain. Res.* **109** 225 (1976)
66. Grillner S, Wallen P *Brain. Res.* **127** 291 (1977)
67. Stein P S G *J. Comp. Physiol.* **124** 203 (1978)
68. Kulagin A S, Shik M L *Biophys.* **15** 171 (1970)
69. Shik M L, Orlovsky G N *Physiol. Rev.* **56** 465 (1976)
70. Forrsberg H et al. *Acta Physiol. Scand.* **100** 283 (1980)
71. Collins J J, Stewart I N *Biol. Cybern.* **68** 287 (1993)
72. Kuramoto Y *Chemical Oscillations Waves and Turbulence* (Berlin: Springer, 1984)
73. Kuramoto Y *Progr. Theor. Phys. Suppl.* **79** 223 (1984)
74. Cohen A H *TINS* **15** 434 (1992)
75. Williams T L et al. *J. Neurophysiol.* **64** 862 (1990)
76. Cohen A H *J. Comp. Physiol. A* **160** 181 (1987)
77. Ermentrout G B, Kopell N *SIAM J. Appl. Math.* **54** 478 (1994)
78. Nishii J, Uno Y, Suzuki R *Biol. Cybern.* **72** 1 (1994)
79. Osovets S M et al. *Usp. Fiz. Nauk* **141** 103 (1983) [*Sov. Phys. Usp.* **26** 801 (1983)]
80. Schuster H G, Wagner P *Biol. Cybern.* **64** 77 (1990)
81. Von der Malsburg C *Internal Report 81-2, Abteilung für Neurobiologie* (Göettingen: MPI für Biophysikalische Chemie, 1981)
82. Von der Malsburg C, Schneider W *Biol. Cybern.* **54** 29 (1986)
83. Livingstone M, Hubel D *Science* **240** 740 (1988)
84. Zeki S, Shipp S *Nature* (*London*) **335** 311 (1988)
85. Eckhorn R et al. *Biol. Cybern.* **60** 121 (1988)
86. Gray C M, Singer W *Proc. Natl. Acad. Sci. USA* **86** 1698 (1989)
87. Engel A K et al. *Eur. J. Neurosci.* **2** 588 (1990)
88. Gray C M et al. Ibid., p. 607
89. Gray C M et al. *Nature* (London) **338** 334 (1989)
90. *Principles of Neural Science* (Eds E R Kandel, J H Schwarz) 2nd edition (New York, Amsterdam, Oxford: Elsevier, 1985)
91. Engel A K, Koenig P, Singer W *Proc. Natl. Acad. Sci. USA* **88** 9136 (1991)
92. Koenig P et al. *Neural Comp.* **7** 469 (1995)
93. Nelson J I et al. *Visual Neurosci.* **9** 21 (1992)
94. Koenig P et al. *Eur. J. Neurosci.* **5** 501 (1993)
95. Ts'o D Y, Gilbert C D *J. Neurosci.* **8** 1712 (1988)
96. Krueger J, Aiple F *J. Neurophysiol.* **60** 798 (1988)
97. Engel A K et al. *Proc. Natl. Acad. Sci. USA* **88** 6048 (1991)
98. Engel A K et al. *Science* **252** 1177 (1991)
99. Chawanya T et al. *Biol. Cybern.* **68** 483 (1993)
100. Knight B W *J. Gen. Physiol.* **59** 734 (1972)
101. Peskin C S *Mathematical Aspects of Heart Physiology* (New York: Courant. Inst. of Math. Sci. Publication, 1975) p. 268
102. Koenig P, Schillen T B *Neural Comp.* **3** 155 (1991)
103. Gerstner W *Phys. Rev. E* **51** 738 (1995)
104. Schillen T B, Koenig P *Neural Comp.* **3** 167 (1991)
105. Sporns O et al. *Neurobiol.* **86** 7265 (1989)
106. Grannan E R, Kleinfeld D, Sompolinsky H *Neural Comp.* **5** 550 (1993)
107. Terman D, Wang D L *Physica D* **81** 148 (1995)
108. Von der Malsburg C, Buhmann J *Biol. Cybern.* **67** 233 (1992)
109. Horn D, Sagi D, Usher M *Neural Comp.* **3** 510 (1991)
110. Meinhardt H, Koch A J *Rev. Mod. Phys.* **66** 1481 (1994)
111. Ivanitskiĭ G R, Medvinskiĭ A B, Tsyganov M A *Usp. Fiz. Nauk* **164** 1041 (1994) [*Phys. Usp.* **37** 961 (1994)]

112. Vasiev B N, Hogeweg P, Parfilov A V *Phys. Rev. Lett.* **73** 3173 (1994)
113. Rabinovich M I, Sushchik M M *Usp. Fiz. Nauk* **160** (1) 3 (1990) [*Sov. Phyf. Usp.* **33** 1 (1990)]
114. Gaponov-Grekhov A V, Rabinovich M I *Nonlinearity in Action* (Heidelberg: Springer, 1991)
115. Bailly C H, Kandel E R *Annu. Rev. Physiol.* **55** 397 (1993)
116. Wang D, Buhmann J, von der Malsburg C *Neural Comp.* **2** 94 (1990)
117. Baird B, Eeckman F, in *Associative Neural Memories. Theory and Implemenation* (Ed. M H Hassoun) (New York, Oxford: Oxford Univ. Press, 1993) p. 135
118. Hopfield J J, Tank D W *Science* **233** 625 (1986)
119. Sompolinsky H, Tsodyks M *Neural Comp.* **6** 642 (1994)
120. Fukai T *Biol. Cybern.* **71** 215 (1994)
121. Rosenblueth A, Cannon W B *Am. J. Physiol.* **135** 349 (1942)
122. Burns D B *The Mammalian Cerebral Cortex* (London: Arnold, 1958)
123. Winfree A T *When Time Breaks Down* (Princeton, New Jersey: Princeton Univ. Press, 1987)
124. Loskutov A Yu, Mikhaĭlov A S *Vvedenie v Sinergetiku* (Introduction to Synergetics) (Moscow: Nauka, 1990)
125. Davidenko J M, Kent P, Jalife J *Physica D* **49** 182 (1991)
126. Downar E et al. *J. Am. Coll. Cardiol.* **4** 703 (1984)
127. Gorelova N A, Bures J *J. Neurobiol.* **14** 353 (1983)
128. Shibata M, Bures J *J. Neurophys.* **35** 381 (1972); **5** 107 (1974)
129. Paullet J E, Ermentrout G B *SIAM J. Appl. Math.* **54** 1720 (1994)
130. Kaplan D T et al. *Math. Biosci.* **90** 19 (1988)
131. Chu P H, Milton J G, Cowan J D *Int. J. Bif. Chaos* **4** 237 (1994)
132. Geisler C D, Goldberg J M *Biophysical J.* **6** 53 (1966)
133. Sholl D A *The Organization of the Cerebral Cortex* (London: Methuen, 1956)
134. Destexhe A *Phys. Rev. E* **50** 1594 (1994)
135. Coullet P, Gil L, Lega J *Physica D* **37** 91 (1989); *Phys. Rev. Lett.* **62** 1619 (1989)
136. Cowan J D, in *Proc. of the founding workshop of the Santa Fe Institute, Santa Fe, New Mexico* (Addison: Wesley, 1987) p. 123
137. Turchin V *Fenomen Nauki* (Phenomenon of Science) (Moscow: Nauka, 1993)
138. Hansel D, Mato G, Meunier C *Neural Comp.* **7** 307 (1995)
139. Connar J A, Walter D, McKown *Biophys.* **18** 81 (1977)
140. Skinner F K, Turrigiano G G, Marder E *Biol. Cybern.* **69** 375 (1993)
141. Ermentrout B, Kopell N *Neural Comp.* **6** 225 (1994)
142. Chay T R, Fan Y S, Lee Y S *Int. J. Bif. Chaos* **5** 595 (1995)
143. Chay T R *Biol. Cybern.* **63** 15 (1990)
144. Golowasch J, Marder E J *Neurophys.* **67** 318 (1992)
145. Golomb D, Guckenheimer J, Gueron S *Biol. Cybern.* **69** 129 (1993)
146. Stein R B et al. *Kybernetic* **15** 1 (1974)
147. FitzHygh R *Biophys. J.* **1** 445 (1961)
148. Nagumo J, Arimoto S, Yoshizawa S *Proc. IRE* **50** 2061 (1962)
149. Bay J S, Hemani H *IEE Trans. Biomed. Eng.* **34** 297 (1987)